

Article

# Ion Pair Dynamics: Solvolyses of Chiral 1,3-Diaryllallyl Carboxylates as a Case Study

Konstantin Troshin, and Herbert Mayr

*J. Am. Chem. Soc.*, **Just Accepted Manuscript** • DOI: 10.1021/ja308670g • Publication Date (Web): 28 Nov 2012

Downloaded from <http://pubs.acs.org> on December 10, 2012

## Just Accepted

"Just Accepted" manuscripts have been peer-reviewed and accepted for publication. They are posted online prior to technical editing, formatting for publication and author proofing. The American Chemical Society provides "Just Accepted" as a free service to the research community to expedite the dissemination of scientific material as soon as possible after acceptance. "Just Accepted" manuscripts appear in full in PDF format accompanied by an HTML abstract. "Just Accepted" manuscripts have been fully peer reviewed, but should not be considered the official version of record. They are accessible to all readers and citable by the Digital Object Identifier (DOI®). "Just Accepted" is an optional service offered to authors. Therefore, the "Just Accepted" Web site may not include all articles that will be published in the journal. After a manuscript is technically edited and formatted, it will be removed from the "Just Accepted" Web site and published as an ASAP article. Note that technical editing may introduce minor changes to the manuscript text and/or graphics which could affect content, and all legal disclaimers and ethical guidelines that apply to the journal pertain. ACS cannot be held responsible for errors or consequences arising from the use of information contained in these "Just Accepted" manuscripts.

# Ion Pair Dynamics: Solvolyses of Chiral 1,3-Diarylallyl Carboxylates as a Case Study

*Konstantin Troshin and Herbert Mayr\**

Department Chemie, Ludwig-Maximilians-Universität München, Butenandtstrasse 5-13

(Haus F), 81377 München, Germany

herbert.mayr@cup.uni-muenchen.de

ABSTRACT. Chiral ion pairs play a key-role in modern enantioselective synthesis though little is known about their properties. We have now used the special features of unsymmetrically substituted allyl derivatives to obtain unprecedented insight in ion pair dynamics. By employing chiral HPLC it was possible to follow the time-dependent concentrations of all four isomeric esters (two regioisomeric pairs of enantiomers) and all four isomeric alcohols generated during the hydrolysis of enantiopure 1-(4-chlorophenyl)-3-phenylallyl and 3-(4-chlorophenyl)-1-phenylallyl 4-nitrobenzoates. Combination of these results with the directly measured rate constant for the reaction of the laser-flash photolytically generated 1-(4-chlorophenyl)-3-phenylallyl cation with water provided a complete mechanistic scheme for allyl carboxylate solvolysis. It is demonstrated that solvolysis and internal return can be explained by the same intermediates. The correlation equation  $\log k = s_N(N + E)$  was used to elucidate the variable importance of external and internal return in the solvolysis reactions. This information will be crucial for the interpretation of the ultrafast dynamics of ion pairs generated by femtosecond laser pulses.

## Introduction

Control of enantioselectivity by noncovalent interactions has become a major tool in organic synthesis. In particular hydrogen bonding, as in thiourea-catalyzed reactions,<sup>1</sup> and ion-pairing<sup>2</sup> have extensively been used for stereoselective transformations. An early example for the use of ion-pairing in asymmetric synthesis was reported by Dolling et al.,<sup>3</sup> who found that a cinchona-derived quarternary ammonium ion salt can be employed as catalyst for the asymmetric methylation of a substituted indanone under phase-transfer conditions. This pioneering work opened the field of asymmetric phase-transfer catalysis, the scope of which has widely been elaborated by Maruoka and associates.<sup>4</sup> Protonation of organic substrates by strong chiral Brønsted acids, in particular BINOL-derived phosphoric acid diesters and their derivatives, gives rise to chiral ion pairs or similar structures, which served as chiral electrophiles in a manifold of reactions,<sup>5</sup> including enantioselective cycloadditions,<sup>6</sup> electrocyclic reactions,<sup>7</sup> 1,4-additions,<sup>8</sup> Friedel-Crafts allylations,<sup>9</sup> reductions,<sup>10</sup> and ene reactions.<sup>11</sup> Hydrogen bonding between the resulting cation and the chiral counteranion often provides additional stabilization of the positively charged electrophilic intermediate and accounts for the augmented enantioselectivity. In some cases it is difficult to differentiate whether chirality is induced by ion-pairing of an achiral cationic electrophile with a chiral counteranion or by activation of neutral electrophiles (e. g., imines or carbonyl compounds) through hydrogen bonding with a chiral Brønsted acid.<sup>12</sup>

However, treatment of prochiral substrates with strong chiral Brønsted acids is not the only method to generate chiral ion pairs for asymmetric counterion-directed synthesis.<sup>2,13</sup> Ion-pairing was also employed in enantioselective iminium-activated reactions by using achiral ammonium ions with chiral counterions<sup>14</sup> as well as in various asymmetric transition-metal-catalyzed reactions, which utilized the directing effect of chiral counteranions.<sup>15</sup> Ooi demonstrated that transition metal complexes with achiral ligands carrying a quarternary onium moiety can electrostatically be bound to chiral anions to induce asymmetrical

1  
2  
3 palladium catalysis.<sup>16</sup> The general importance of ion-pairing in transition metal-catalyzed  
4  
5 reactions has been reviewed by Macchioni who suggested that ion-pairing should be  
6  
7 considered as one of the instruments for tuning catalytic processes.<sup>17</sup>  
8  
9

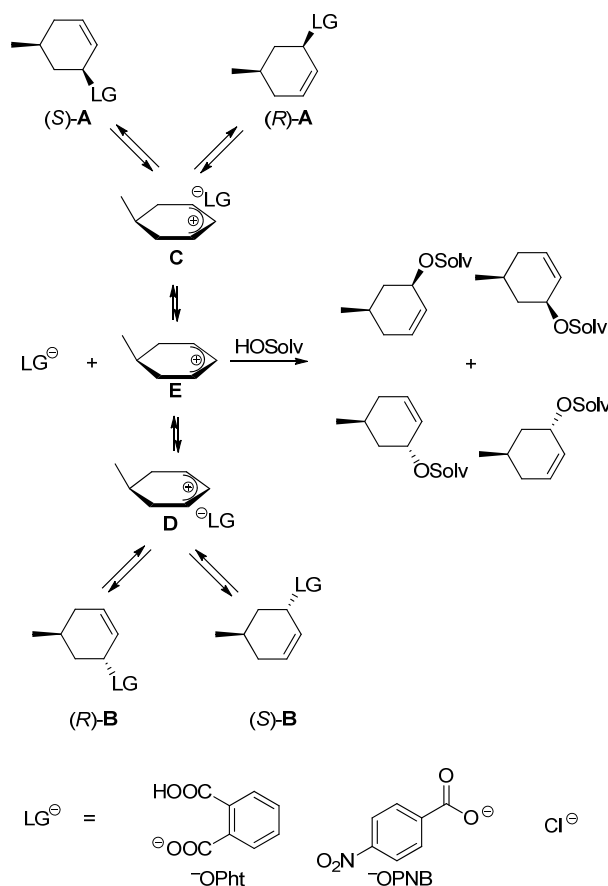
10 Enantioselective catalysis was furthermore achieved by combining ion-pairing with hydrogen  
11  
12 bonding. Examples are reactions catalyzed by chiral ureas which are coordinated to achiral  
13  
14 counterions<sup>18</sup> as well as cooperative catalysis, where hydrogen bonding was used to link the  
15  
16 complex counterion to the active intermediate, thus providing additional attractive forces  
17  
18 within the ion pair.<sup>19</sup> Extensive studies on the role of ion-pairing in carbocationic  
19  
20 polymerizations have recently been reviewed by Bochmann.<sup>20</sup>  
21  
22  
23

24 While the targeted use of ion-pairing in enantioselective synthesis and polymerization  
25  
26 reactions thus reflects recent developments, the importance of ion-pairing for organic  
27  
28 reactivity has already been recognized in the 1950s by Winstein and coworkers. Their studies  
29  
30 of S<sub>N</sub>1 solvolyses<sup>21</sup> provide the basis of our current understanding of ion pairs and their  
31  
32 reactivities.<sup>22</sup> Because of their ability to undergo allylic rearrangements, allyl derivatives  
33  
34 turned out to be particularly valuable systems for gaining insight in the nature and reactivities  
35  
36 of ion pairs.<sup>21a,22,23</sup> Goering's pioneering investigations of the transformations of optically  
37  
38 active allyl derivatives by titrimetric and polarimetric methods as well as product analyses  
39  
40 including isotope exchange experiments have become text-book examples<sup>24</sup> to demonstrate  
41  
42 the role of ion-pairing in S<sub>N</sub>1 reactions.  
43  
44  
45  
46  
47

48 Since the *cis/trans* isomerization of optically active *cis*- and *trans*-5-methylcyclohex-2-enyl 2-  
49  
50 carboxybenzoates (**A**  $\rightleftharpoons$  **B**, LG = OPht, Scheme 1) in acetonitrile was found to proceed  
51  
52 significantly more slowly than the racemization ((*S*)-**A**  $\rightleftharpoons$  (*R*)-**A**; (*S*)-**B**  $\rightleftharpoons$  (*R*)-**B**),<sup>25</sup>  
53  
54 Goering proposed the formation of ion pair intermediates (**C**, **D**), in which the anion remains  
55  
56 on the same face of the allyl cation as in the substrate. The collapse of these ion pairs (internal  
57  
58 return) either regenerates the starting materials or leads to their enantiomers by attack of the  
59  
60 anion at the other allylic terminus. The *cis/trans*-isomerization, which requires the migration

of the leaving group to the other face of the allyl cation, was proposed to proceed via dissociation of the initial ion pairs to an achiral carbocationic intermediate (**E**) that can be attacked by the leaving group from both faces (Scheme 1).<sup>25</sup>

**Scheme 1.** Ion Pair Mechanism Proposed by Goering for Solvolyses and Rearrangements of *cis*- and *trans*-5-Methyl-cyclohex-2-enyl Derivatives<sup>a</sup>



<sup>a</sup> The descriptors (*R*) and (*S*) for the configuration of C-5 (connected to the methyl group) are omitted.

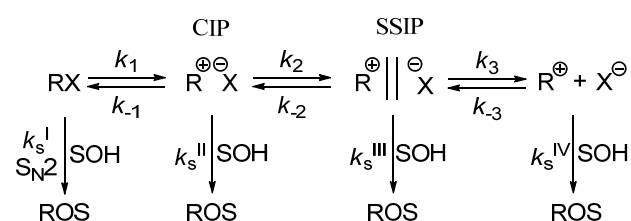
The hydrolyses of *cis*- and *trans*-5-methylcyclohex-2-enyl 2-carboxybenzoates (**A**, **B**, LG = OPht)<sup>26</sup> and 4-nitrobenzoates (**A**, **B**, LG = OPNB)<sup>27</sup> in aqueous acetone as well as the ethanolyses and acetolyses of *cis*- and *trans*-5-methylcyclohex-2-enyl chlorides (**A**, **B**, LG = Cl)<sup>28</sup> were rationalized on the basis of this mechanism. In none of these cases *cis/trans* isomerization of the non-reacted substrates was detected, and the polarimetric rate constant

(racemization plus solvolysis) was always larger (factor of 1.1 to 5.07) than the titrimetric rate constant (solvolysis only).

In contrast to the situation described for symmetrical allyl systems in Scheme 1, racemization of unsymmetrical allyl derivatives implies migration of the leaving group to the other face of the allyl cation. As solvolyses of *trans*-3-methyl-1-phenylallyl and *trans*-1-methyl-3-phenylallyl 4-nitrobenzoates in aqueous acetone were later observed to be accompanied by approximately 70% racemization of the unsolvolyzed esters, Goering concluded that the previously investigated stereochemical behavior of cyclohexenyl derivatives (Scheme 1) was largely dominated by conformational phenomena, which are absent in acyclic derivatives.<sup>29</sup> The stereochemistry of S<sub>N</sub>1 reactions of acyclic allyl derivatives, which is crucial for the understanding of ion-pairing in general, has, therefore, not conclusively been clarified up to the present time.

Winstein's ion pair mechanism (Scheme 2),<sup>30</sup> which has commonly been used to rationalize the course of solvolysis reactions through the intermediacy of contact ion pairs (CIP), solvent separated ion pairs (SSIP), and free ions, has recently been employed to interpret the picosecond dynamics of laser-flash-generated contact ion pairs.<sup>31</sup>

**Scheme 2.** Classical Winstein Scheme for Solvolysis Reactions.<sup>30</sup>



It is commonly assumed that such photolytically generated contact ion pairs, which may either be formed directly as the initial cleavage products or through electron transfer in the initially generated geminate radical pairs, are similar to the intermediates in solvolysis

1  
2  
3 reactions.<sup>31</sup> Vice versa, the rates measured for geminate recombinations of laser-flash  
4  
5 photolytically generated ion pairs, were used to discuss structural effects on the rates of  
6  
7 internal return during the solvolytic reactions.<sup>32</sup>  
8  
9

10 However, Winstein's solvolysis scheme includes many parameters which could not be  
11  
12 unambiguously differentiated with the analytical methods available at that time so that many  
13  
14 questions remained open. It is still unclear, for example, whether solvolysis and internal return  
15  
16 proceed through the same intermediates or are two independent processes involving different  
17  
18 types of ion pairs.<sup>33</sup>  
19  
20

21 A crucial step toward a quantitative description of solvolysis reactions, and of nucleophilic  
22  
23 aliphatic substitutions in general, were the investigations of Jencks, Richard, and Tsuji,<sup>34-36</sup>  
24  
25 who used clock-methods to determine rate constants for the attack of solvents on the  
26  
27 intermediate carbocations. These authors were not only able to identify the change from S<sub>N</sub>1  
28  
29 to S<sub>N</sub>2 mechanisms<sup>34</sup> but also clarified the dynamics of ion pair dissociation<sup>35</sup> and  
30  
31 recombination.<sup>36</sup>  
32  
33

34 By introducing stopped-flow techniques for determining rates of solvolysis reactions, which  
35  
36 occur in the millisecond to second time domain,<sup>37</sup> and systematic extension of the data set for  
37  
38 the rates of the reactions of carbocations with solvents<sup>38</sup> and other nucleophiles,<sup>39</sup> we arrived  
39  
40 at linear free energy relationships,<sup>39,40</sup> which allow one to predict changes of solvolysis  
41  
42 mechanisms as the substrates and solvents are altered.<sup>41</sup> Under the same conditions,  
43  
44 increasing stabilization of the carbocations led to the change from S<sub>N</sub>2 reactions, over S<sub>N</sub>1  
45  
46 reactions without and with common ion return, to S<sub>N</sub>2C<sup>+</sup> processes (formation of carbocation  
47  
48 occurs faster than its reaction with the solvent) and heterolytic cleavages of esters which  
49  
50 proceed with formation of persistent carbocations.<sup>41</sup> Furthermore, we have recently employed  
51  
52 femtosecond spectroscopy to investigate the dynamics of free and paired carbocations on the  
53  
54 picosecond time scale in collaboration with the Riedle group.<sup>42</sup>  
55  
56  
57  
58  
59  
60

1  
2  
3 Combination of all these techniques has provided detailed information about the whole range  
4 of carbocation reactivities<sup>37,43</sup> – from very slow reactions to those occurring within ion pairs  
5 which proceed at rates approaching vibrational frequencies. On the other hand, our knowledge  
6 about structures and dynamics of intramolecular interconversions of ion pairs has remained  
7 crude.  
8  
9

10 We, therefore, approached the dynamics of ion pair transformations by taking advantage of  
11 the special properties of allylic derivatives described above. While titrimetry and polarimetry  
12 were the most important analytical tools available to Goering for studying the course of the  
13 solvolysis reactions, we now employed chiral HPLC techniques to obtain unprecedented  
14 insights in the course of S<sub>N</sub>1 reactions and ion-pairing.  
15  
16

17 When the enantiopure esters (*R*)-**1** or (*S*)-**2** were dissolved in aqueous acetone (for structures  
18 see Scheme 3), mixtures of four isomeric allyl alcohols (hydrolysis products) and of four  
19 isomeric allyl 4-nitrobenzoates (starting material and products of ion recombination) were  
20 obtained. As we succeeded in separating these eight compounds by HPLC, it was possible to  
21 follow the concentrations of each of these individual compounds as a function of time and  
22 develop a kinetic model, which quantitatively describes the whole mechanistic scheme. As we  
23 will report individual rate constants for interconversions between covalent substrates, ion  
24 pairs, and free ions, this work can be considered as a bridge between the classical solvolysis  
25 studies of the 1950s to 1970s and modern applications of ion-pairing in stereoselective  
26 organic synthesis and their role in photosolvolytic processes. We, thus, can not only answer  
27 questions which remained open when our knowledge of ion pairing effects in solvolysis  
28 reactions was mostly derived from the difference between polarimetric and titrimetric rate  
29 constants, but also provide the basis for the interpretation of ultrafast dynamics of ion pairs  
30 generated by femtosecond laser pulses.  
31  
32  
33  
34  
35  
36  
37  
38  
39  
40  
41  
42  
43  
44  
45  
46  
47  
48  
49  
50  
51  
52  
53  
54  
55  
56  
57  
58  
59  
60

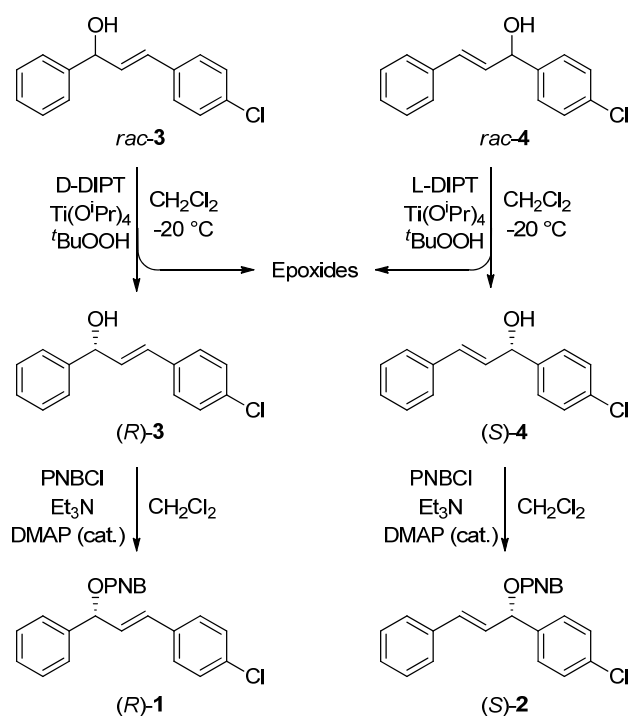


## Results

### Synthesis and Chromatographic Separation of the Model Compounds

The regioisomeric alcohols *rac*-**3** and *rac*-**4** were obtained by NaBH<sub>4</sub> reduction of the corresponding chalcones according to ref 44. Sharpless kinetic resolution<sup>45</sup> of (*rac*)-**3** and *rac*-**4** using D- or L-diisopropyltartrate (D-/L-DIPT), respectively, followed by treatment with 4-nitrobenzoyl chloride in the presence of triethylamine and recrystallization gave the enantiopure (ee > 99%, HPLC) allylic esters (*R*)-**1** and (*S*)-**2** (Scheme 3).

**Scheme 3.** Synthesis of the Enantiopure Allylic Esters (*R*)-**1** and (*S*)-**2** (PNB = 4-nitrobenzoyl, DIPT = diisopropyltartrate, DMAP = 4-(dimethylamino)pyridine).



As treatment of either (*R*)-**1** or (*S*)-**2** with aqueous acetone may give a mixture of four esters [(*R*)-**1**, (*S*)-**1**, (*R*)-**2**, and (*S*)-**2**] and of four alcohols [(*R*)-**3**, (*S*)-**3**, (*R*)-**4**, and (*S*)-**4**], a complete analysis of the solvolysis mechanism requires monitoring of the concentrations of eight compounds.

Figure 1 shows that mixtures of the racemic compounds **1–4** can be resolved using chiral HPLC (eight peaks in total), which gives the unique possibility of following the time-dependent concentrations of the individual enantiomers.

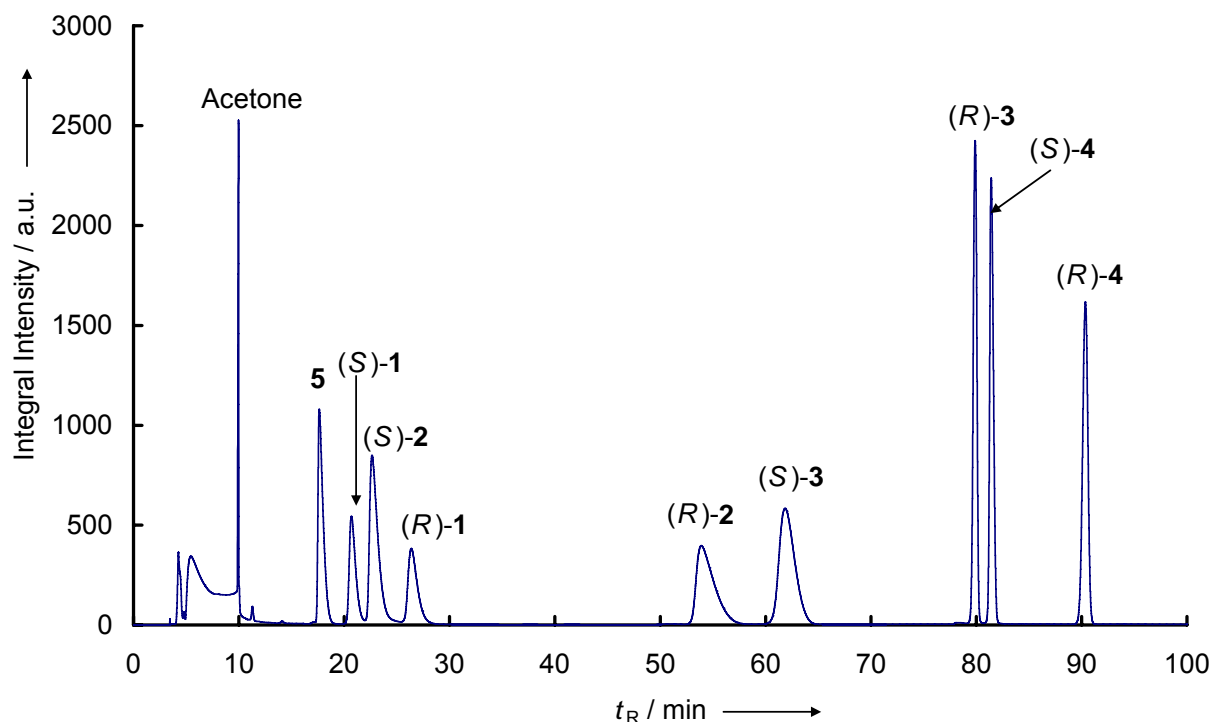


**Figure 1.** Chromatogram of an artificial mixture of racemic **1–4** and (*E*)-1-(4-methylphenyl)-3-phenylprop-2-en-1-one (**5**) (internal standard). Details of the HPLC method are described in the Supporting Information.

## Kinetic experiments

**General.** The 4-nitrobenzoates **1** and **2** were solvolyzed in aqueous acetone at 25 °C with and without addition of various nucleophiles (the experiments are summarized in Table 1).

**Table 1.** Summary of the HPLC kinetic experiments.

entry	solvent	substrate	[substrate] <sub>0</sub> / M	additive	[additive] <sub>0</sub> / M
1	60 % aq acetone	( <i>R</i> )- <b>1</b>	$1.53 \times 10^{-3}$	-	-
2	60 % aq acetone	( <i>R</i> )- <b>1</b>	$8.04 \times 10^{-4}$	Bu <sub>4</sub> NOPNB <sup>a</sup>	$4.82 \times 10^{-3}$
3	60 % aq acetone	( <i>R</i> )- <b>1</b>	$7.82 \times 10^{-4}$	Bu <sub>4</sub> NOPNB <sup>a</sup>	$5.25 \times 10^{-2}$
4	60 % aq acetone	( <i>R</i> )- <b>1</b>	$8.04 \times 10^{-4}$	NaN <sub>3</sub>	$7.08 \times 10^{-2}$
5	60 % aq acetone	( <i>R</i> )- <b>1</b>	$1.02 \times 10^{-3}$	Bu <sub>4</sub> NCl	$1.87 \times 10^{-2}$
6	60 % aq acetone	( <i>R</i> )- <b>1</b>	$8.51 \times 10^{-4}$	Bu <sub>4</sub> NCl	$1.01 \times 10^{-1}$
7	60 % aq acetone	( <i>R</i> )- <b>1</b>	$8.70 \times 10^{-4}$	Piperidine	$5.42 \times 10^{-2}$
8	60 % aq acetone	( <i>R</i> )- <b>1</b>	$8.61 \times 10^{-4}$	LiClO <sub>4</sub>	$9.46 \times 10^{-3}$
9	60 % aq acetone	( <i>S</i> )- <b>2</b>	$7.85 \times 10^{-4}$	-	-
10	60 % aq acetone	( <i>S</i> )- <b>2</b>	$7.90 \times 10^{-4}$	NaN <sub>3</sub>	$7.66 \times 10^{-2}$
11	80 % aq acetone	( <i>R</i> )- <b>1</b>	$7.72 \times 10^{-4}$	-	-
12	90 % aq acetone	( <i>R</i> )- <b>1</b>	$6.82 \times 10^{-4}$	-	-

<sup>a</sup> Tetrabutylammonium 4-nitrobenzoate

Aliquots of the reaction mixtures were extracted with dichloromethane or diethyl ether after certain time intervals followed by HPLC analysis. A typical chromatogram obtained during such an experiment is shown in Figure S1 of the Supporting Information. By using (*E*)-1-(4-methylphenyl)-3-phenylprop-2-en-1-one (**5**) as internal standard, we have determined the time-dependent yields for all compounds present in the mixture.

**Solvolyses of (*R*)-**1** and (*S*)-**2** in 60% Aqueous Acetone.** Figure 2 shows that both regioisomeric alcohols **3** and **4** are formed as racemates during the solvolysis of (*R*)-**1** in 60% aq acetone. The marginal separation of the graphs for (*R*)-**3** and (*S*)-**3** can be explained by the different shapes of their HPLC signals, and the drift of the baseline caused by the gradient used to shorten the overall elution time. As no isomerization was detectable within 2.75 h when (*S*)-**4** was dissolved in 60% aq acetone containing 2 mM of 4-nitrobenzoic acid (the highest concentration of the acid which can be present at the end of the solvolyses under the experimental conditions used), one can exclude enantioselective formation of **3** and **4** and subsequent isomerization. In line with this observation, the ratio [**3**]/[**4**] = 1.5 remained constant throughout the reaction. An S<sub>N</sub>2 mechanism as well as nucleophilic trapping of the

chiral contact ion pairs (CIPs) by water prior to racemization (steps with  $k_s^I$  and  $k_s^{II}$  in the classical Winstein scheme<sup>30</sup>) can, therefore, be excluded for this system: both pathways would result in the formation of enantioenriched products (complete or partial inversion of the configuration).

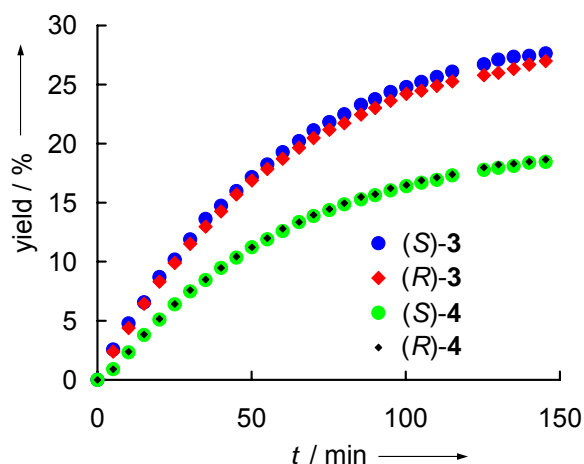


**Figure 2.** Time-dependent yields of **3** and **4** during the solvolysis of (*R*)-**1** (1.5 mM) in 60% aqueous acetone at 25°C.

Figure 3 shows that the consumption of (*R*)-**1** does not only lead to the formation of the hydrolysis products **3** and **4** discussed above but also to the intermediate appearance of the isomeric 4-nitrobenzoates (*S*)-**2**, (*S*)-**1**, and (*R*)-**2**.

The prevailing formation of (*S*)-**2** indicates that the leaving group stays preferentially at the same face of the plane of the allyl cation which implies that allylic rearrangement occurs predominantly at the contact ion pair stage.

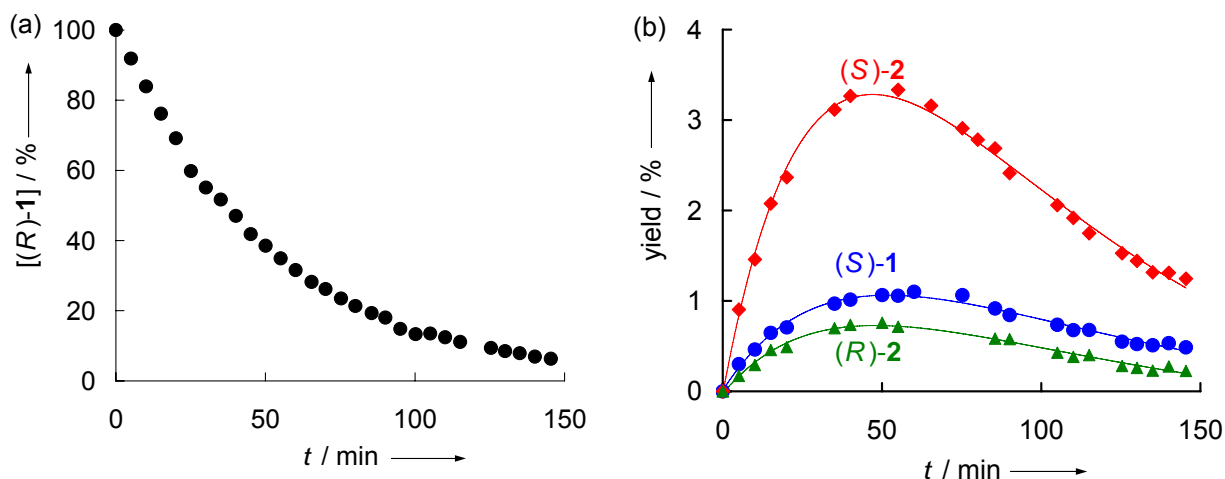
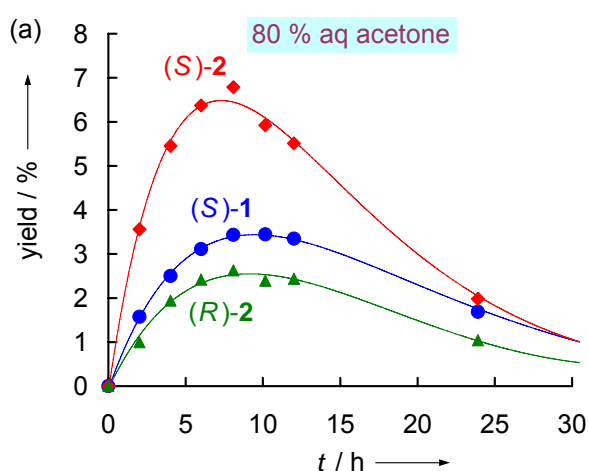


**Figure 3.** Time-dependent yields of (a) (R)-1 and (b) (S)-2, (S)-1, and (R)-2 during solvolysis of (R)-1 (1.5 mM) in 60% aq acetone, 25 °C.

Solvolysis of (S)-2 in 60% aqueous acetone followed exactly the same pattern as the solvolysis of (R)-1 in the same solvent. Both alcohols **3** and **4** were formed as racemates, and the ratio  $[\mathbf{3}]/[\mathbf{4}] = 1.5$  is the same as in the solvolysis of (R)-1. One can, therefore, conclude that the same achiral intermediates are responsible for the formation of the alcohols **3** and **4** from both precursors **1** and **2**. As addition of 9.5 mM  $\text{LiClO}_4$  had no noticeable effect on the time-dependent concentrations of **1-4** during the solvolysis of (R)-1 in 60% aq acetone (see pp S44-S46 of the Supporting Information), the participation of SSIPs cannot play a significant role (otherwise special salt effect<sup>30</sup> would be expected). Therefore, the alcohols **3** and **4** must be formed via the free 1-(4-chlorophenyl)-3-phenylallylium ions (**6**) or through ion pairs which interconvert more rapidly via **6** than they react with water. The preferred formation of **3** over **4** can be explained by the charge distribution in **6** and does not reflect the relative thermodynamic stabilities of **3** and **4** (a ratio of  $[\mathbf{3}]/[\mathbf{4}] = 0.88$  was obtained by equilibration in the presence of *p*-toluenesulfonic acid, see p S57 of the Supporting Information for details). According to NBO calculations (see p S96 of the Supporting Information for details), the positive charge is greater on the phenyl-substituted allyl terminus of the 1,3-diarylallyl cation, as phenyl stabilizes carbocations better than 4-chlorophenyl. These observations are

consistent with results obtained by Easton et al. for other unsymmetrical allyl derivatives.<sup>46</sup> The stereospecificity of the allylic rearrangement of (*S*)-**2** in 60% aqueous acetone is also analogous to the previous case: (*R*)-**1** is the major isomerization product followed by (*S*)-**1** and (*R*)-**2** (Figure S30 of the Supporting Information).

**Solvolysis of (*R*)-**1** in 80 and 90% Aqueous Acetone.** The rate of consumption of (*R*)-**1** in acetone-water mixtures decreases from 60% to 80% and 90% aq acetone ( $k_{\text{rel}} = 73$ , 7, and 1, respectively) as expected from the solvent ionizing power  $Y$ .<sup>47</sup> Figure 4 shows that the yield of rearranged esters increases considerably with decreasing water content in the solvent and that the sequence  $[(S)\text{-}\mathbf{2}] > [(S)\text{-}\mathbf{1}] > [(R)\text{-}\mathbf{2}]$  does not change, which can be explained by decreasing dissociation abilities of the solvents ( $\epsilon_r$ )<sup>48</sup> and increasing nucleophilicities of <sup>-</sup>OPNB from 60% to 80% and 90% aq acetone (as observed for acetate anion<sup>37</sup>).



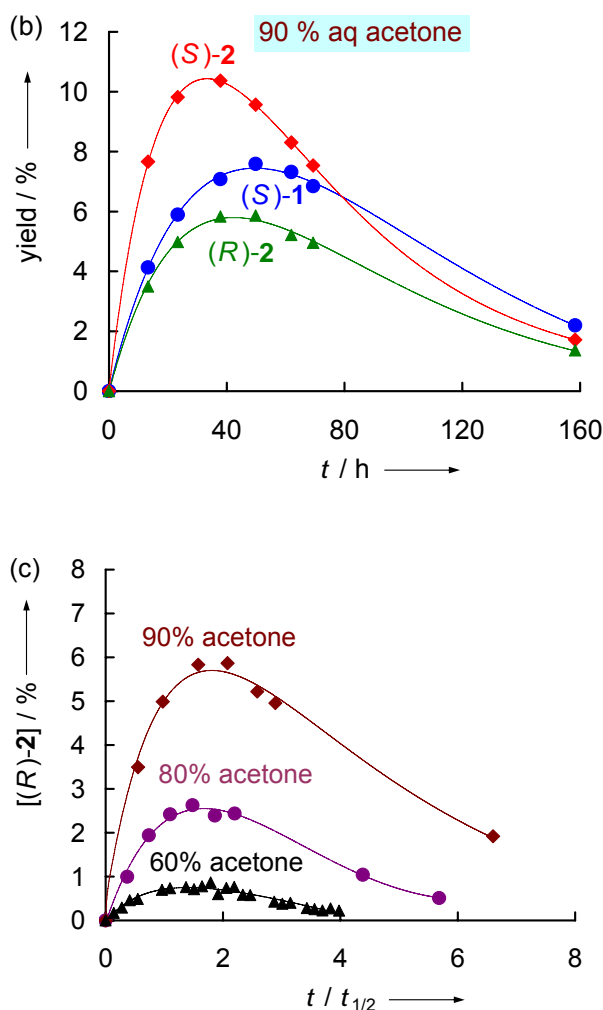


**Figure 4.** Time-dependent yields of (S)-2, (S)-1, and (R)-2 during solvolysis of (R)-1 in (a) 80% aq acetone ( $[(R)-1]_0 = 0.77$  mM) and (b) 90% aq acetone ( $[(R)-1]_0 = 0.68$  mM) as well as (c) yields of (R)-2 during solvolyses of (R)-1 in 60 ( $[(R)-1]_0 = 1.5$  mM), 80 ( $[(R)-1]_0 = 0.77$  mM), and 90% ( $[(R)-1]_0 = 0.68$  mM) aq acetone.<sup>49</sup>

**Solvolysis of (R)-1 in the Presence of External Nucleophiles.** When the solvolysis of (R)-1 in 60% aqueous acetone was performed in the presence of piperidine (54.2 mM), 40% of the allyl cations **6** were intercepted by the amine leading to the formation of the regioisomeric (E)-1,3-diarylallylpiperidines in ca 1:1 ratio (<sup>1</sup>H NMR), and the total yield of the alcohols decreased to ca 60%. Non-regioselective formation of 1,3-diarylallylpiperidines can be explained by diffusion-controlled reaction of piperidine with both allylic termini of the cation,

which is in agreement with the prediction based on reactivity parameters of piperidine and **6**.<sup>50</sup> The same product ratio was found for the reaction of piperidine with the free cation **6** in dichloromethane (see p S6 of the Supporting Information for details).

In the presence of sodium azide (70.8 mM), allyl azide was the major product of the solvolysis reaction of (*R*)-**1** in 60% aqueous acetone, and the total yield of **3** and **4** was only about 3%. These observations show that the intermediates, which give rise to the formation of **3** and **4**, can almost quantitatively be intercepted by external nucleophiles, which is in agreement with the hypothesis that these intermediates are free 1,3-diarylallyl cations **6**. On the other hand, the various isomerization pathways of (*R*)-**1** were differently affected by external nucleophiles. The yield of (*S*)-**2**, which reached a maximum of 3.2% in the absence of nucleophiles, was only slightly reduced to 2.6% in the presence of piperidine (54.2 mM), and to 2.4% in the presence of NaN<sub>3</sub> (70.8 mM). In contrast, the same concentrations of NaN<sub>3</sub> reduced the formation of (*S*)-**1** by a factor of 2.2 (Figure 5), and [(*R*)-**2**] levels below the detection limit (not shown in Figure 5, see Figure S24a). An analogous situation was observed for the solvolysis of (*S*)-**2** in the presence of 76.6 mM NaN<sub>3</sub> (Figure S33 of the Supporting Information).

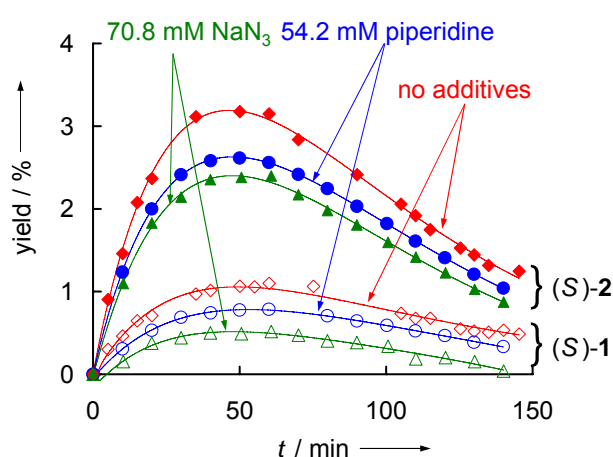
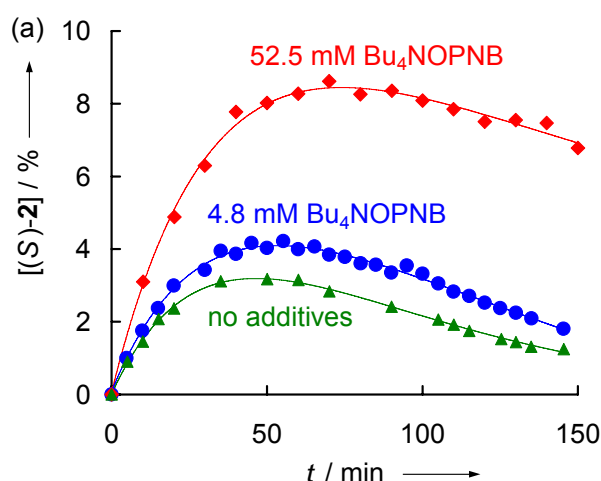


**Figure 5.** Time-dependent yields of (*S*)-**2** (filled points) and (*S*)-**1** (open points) generated during solvolysis of (*R*)-**1** (0.80 – 1.5 mM) without and with added nucleophiles (60% aq acetone, 25 °C).



Addition of chloride ions reduced the yields of the rearranged diarylallyl 4-nitrobenzoates (*S*)-**1**, (*S*)-**2** and (*R*)-**2** to similar extents (Supporting Information, Figures S19 and S22). Since the 1,3-diarylallyl chlorides formed by trapping of the free cation **6** by  $\text{Cl}^-$  undergo fast dissociation to regenerate **6**, the yields of the hydrolysis products **3** and **4** were not affected, however.

**Solvolysis of (*R*)-**1** in the Presence of Tetrabutylammonium 4-Nitrobenzoate (Common Ion Return).** Small amounts of  $\text{Bu}_4\text{NOPNB}$  (4.8 mM) reduced the rate of consumption of [(*R*)-**1**] in 60% aq acetone by only 7% (Figure S9a of the Supporting Information), while the yields of (*S*)-**2** (Figure 6a), (*R*)-**2** (Figure 6b) and (*S*)-**1** (Figure 6c) increased by factors of 1.3, 2.5 and 2, respectively. When a high concentration of  $\text{Bu}_4\text{NOPNB}$  (52.5 mM) was present, the consumption of (*R*)-**1** became significantly slower (factor of 0.65, common ion rate depression), and the yield of (*S*)-**2** increased by a factor of 2.5 (Figure 6a), while the yields of (*R*)-**2** and (*S*)-**1** were approximately 8 (Figure 6b) and 6.5 (Figure 6c) times higher than in the absence of 4-nitrobenzoate. In summary,  $\text{Bu}_4\text{NOPNB}$  additives increased the yields of (*R*)-**2** and (*S*)-**1** by a significantly higher factor than the yield of (*S*)-**2**.



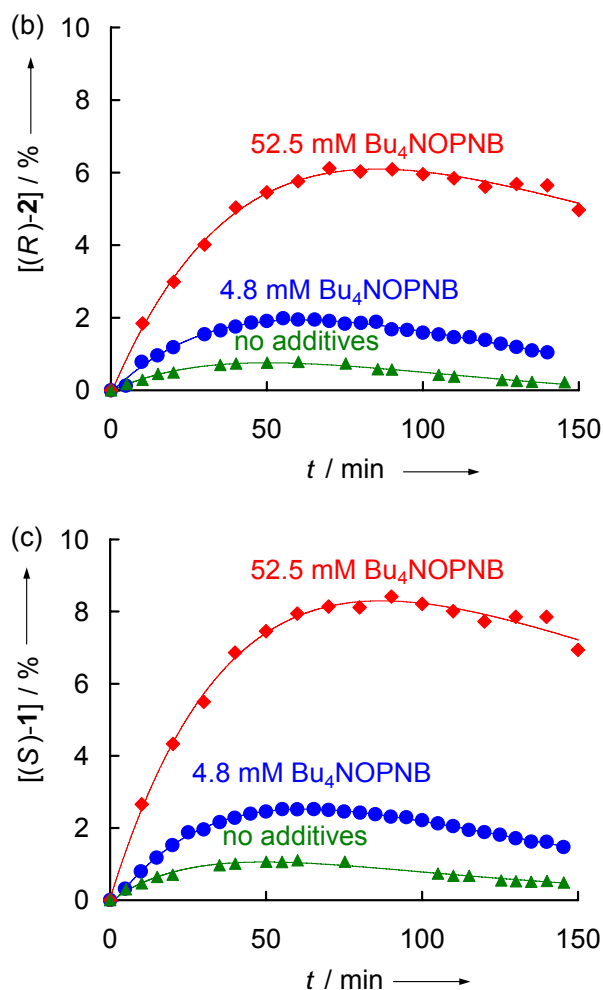
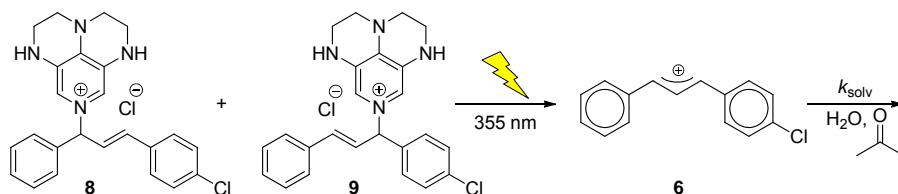


**Figure 6.** Time-dependent yields of (a) (S)-2, (b) (R)-2, and (c) (S)-1 generated during solvolysis of (R)-1 (0.78– 1.5 mM) in the presence of various amounts of Bu<sub>4</sub>NOPNB (60% aq acetone, 25 °C).

**Reaction of the Diarylallyl Cation **6** with Water in Aqueous Acetone.** In order to put the trapping reactions of the intermediate diarylallyl cation **6** on an absolute scale, we have directly measured the rate of consumption of laser flash photolytically generated **6** in 60% aq acetone. As acetone has strong absorption in the UV region, excitation at  $\lambda < 310$  nm, as used in routine laser flash experiments,<sup>42</sup> was not possible. For that reason, a modified procedure<sup>51</sup> using a mixture of SuperDMAP-derived salts **8** and **9** which can be excited at 355 nm was applied (Scheme 4).

**Scheme 4.** Laser Flash Photolytic Generation of the 1,3-Diaryllallyl Cation **6** in 60% aq Acetone.



The reaction with water was followed spectrophotometrically at the absorption maximum of **6** (510 nm), and the rate constant for the reaction of **6** with water ( $k_{\text{solv}} = 1.34 \times 10^7 \text{ s}^{-1}$ ) was obtained by fitting the time-dependent absorbance to the monoexponential function  $A_t = A_0 e^{-k_{\text{solv}} t} + C$ . As the  $k_{\text{solv}}$  values obtained at three different precursor concentrations agreed within the experimental error range ( $\pm 5\%$ ), the influence of the photoleaving group or impurities, which might be present in the stock solution of the precursors, on the reaction kinetics can be excluded.

## Discussion

Let us now develop a mechanistic scheme which accounts for the experimental findings. The observation that (*S*)-**2** is the preferred rearrangement product during the solvolysis of (*R*)-**1**, and vice versa, (*R*)-**1** is the preferred rearrangement product during the solvolysis of (*S*)-**2** indicates that there is a special pathway interconnecting these two isomers. Can it be a 1,3-sigmatropic rearrangement that avoids the intermediate formation of allyl cations?

If this were the case, decreasing solvent ionizing power,<sup>47</sup> i.e., changing from 60% aqueous acetone to 80 and 90% aqueous acetone should decrease the yields of esters formed by ionic pathways relative to those generated by a sigmatropic rearrangement. Comparison of Figures 3b, 4a, and 4b shows that the ratio  $[(S)\text{-}2]/([(S)\text{-}1] + [(R)\text{-}2])$  even decreases in less ionizing

solvents, which clearly rules out a sigmatropic rearrangement of (*R*)-**1** into (*S*)-**2** and vice versa.

In line with Goering's observations for cyclic allyl cations, we, therefore, conclude that the preferred isomerization (*R*)-**1** → (*S*)-**2** proceeds via suprafacial migration of the carboxylate anion at the contact ion pair stage.

Figure 5 shows that the addition of NaN<sub>3</sub> (70.8 mM) and piperidine (54.2 mM) reduces the yield of (*S*)-**2** to a much smaller extent (factors of 1.3 and 1.2, respectively) than that of (*S*)-**1** (factors of 2.2 and 1.5, respectively). (*R*)-**2** shows a similar behavior as (*S*)-**1** (Figure S24a of the Supporting Information). Cl<sup>−</sup> ions exert similar effects (Figure S19a of the Supporting Information). Vice versa, the addition of 4.8 mM Bu<sub>4</sub>NOPNB increases the maximum concentration of (*S*)-**2** by a factor of only 1.3 (Figure 6a), while the concentrations of (*R*)-**2** (Figure 6b) and (*S*)-**1** (Figure 6c) grow by factors of 2 to 2.5.

These observations indicate that the isomerizations of the 4-nitrobenzoates (*R,S*)-**1** as well as of (*R,S*)-**2** proceed via two different pathways: one, which is affected by external nucleophiles (including common ions, external return<sup>52</sup>), and one which is not affected by the presence of external nucleophiles (internal return). The preferred rearrangement of (*R*)-**1** into (*S*)-**2**, where the leaving group stays on the same face of the allyl cation, is rationalized by internal return, which is not 100% stereospecific, however, because part of (*S*)-**1** and (*R*)-**2** must also arise from internal return. The latter conclusion is derived from the observation that 70.8 mM NaN<sub>3</sub> reduces the yield of (*S*)-**1** at the maximum of the curve in Figure 5 to 45% of the value observed in the absence of additives, while the same concentration of azide ions reduces the total yield of the hydrolysis products **3** and **4** from 100% to 3%. If (*S*)-**1** would exclusively be formed through external return, i.e., by trapping of **6** by <sup>−</sup>OPNB, the yield of (*S*)-**1** should be reduced by a factor of 30, as the yields of the alcohols **3** and **4**.

The isomer (*R*)-**2** shows a similar behavior as (*S*)-**1**, but a precise evaluation of the small quantities of (*R*)-**2** is problematic because of the broadness of the HPLC peak of this isomer

(Figure 1). Complementary observations were made for the solvolysis of (*S*)-**2** (see pp S50-S51 of the Supporting Information for details). We, therefore, conclude that the rearrangements through ion pairs do not only proceed via suprafacial migration of carboxylate anion but also via migration of the carboxylate anion to the other face of the allyl cation without dissociation to the free ions.

Table 2 shows that the time-dependent difference  $\Delta_t = [(S)\text{-}\mathbf{2}]_t - [(R)\text{-}\mathbf{2}]_t$  is independent (within experimental error) of the nature and concentration of the external nucleophile. If external nucleophiles were able to attack the CIPs, the value of  $\Delta_t$  could not be nucleophile-independent. One can, therefore, conclude that the CIPs generated in this system are inert to any additive used in the present work, including strong nucleophiles such as  $\text{N}_3^-$ .

**Table 2.** Difference  $\Delta_t = [(S)\text{-}\mathbf{2}]_t - [(R)\text{-}\mathbf{2}]_t$  at Certain Reaction Times During Solvolysis of (*R*)-**1** in the Presence of Various Additives (60% Aq Acetone, 25 °C).

Additive	$\Delta_t$				
	at 10 min	at 20 min	at 40 min	at 50 min	at 60 min
None	1.2	1.9	2.5	2.4	2.4
5 mM $\text{Bu}_4\text{NOPNB}$	1.0	1.8	2.1	2.1	2.0
52.5 mM $\text{Bu}_4\text{NOPNB}$	1.3	1.9	2.7	2.6	2.5
54 mM piperidine	1.1	1.8	2.5	2.6	2.4
70.8 mM $\text{NaN}_3$	1.1	1.8	2.4	2.4	2.4

These observations exclude the solvolysis mechanism proposed by Dvorko et al.<sup>53</sup> who assumed that the azide anion generally attacks the contact ion pairs rather than SSIPs or CSIPs (cavity separated ion pairs), which are proposed by Dvorko to be intermediates on the way from CIP to SSIP in Scheme 2.

As discussed above, the formation of (*S*)-**1** and (*R*)-**2** from (*R*)-**1** can be suppressed by strong nucleophiles, such as  $\text{NaN}_3$ , by more than 50 %. Internal return, therefore, is not the major pathway for the formation of these isomers, and external return<sup>52</sup> must be their main source, particularly when the reactions are carried out in the presence of  $\text{Bu}_4\text{NOPNB}$ . A similar

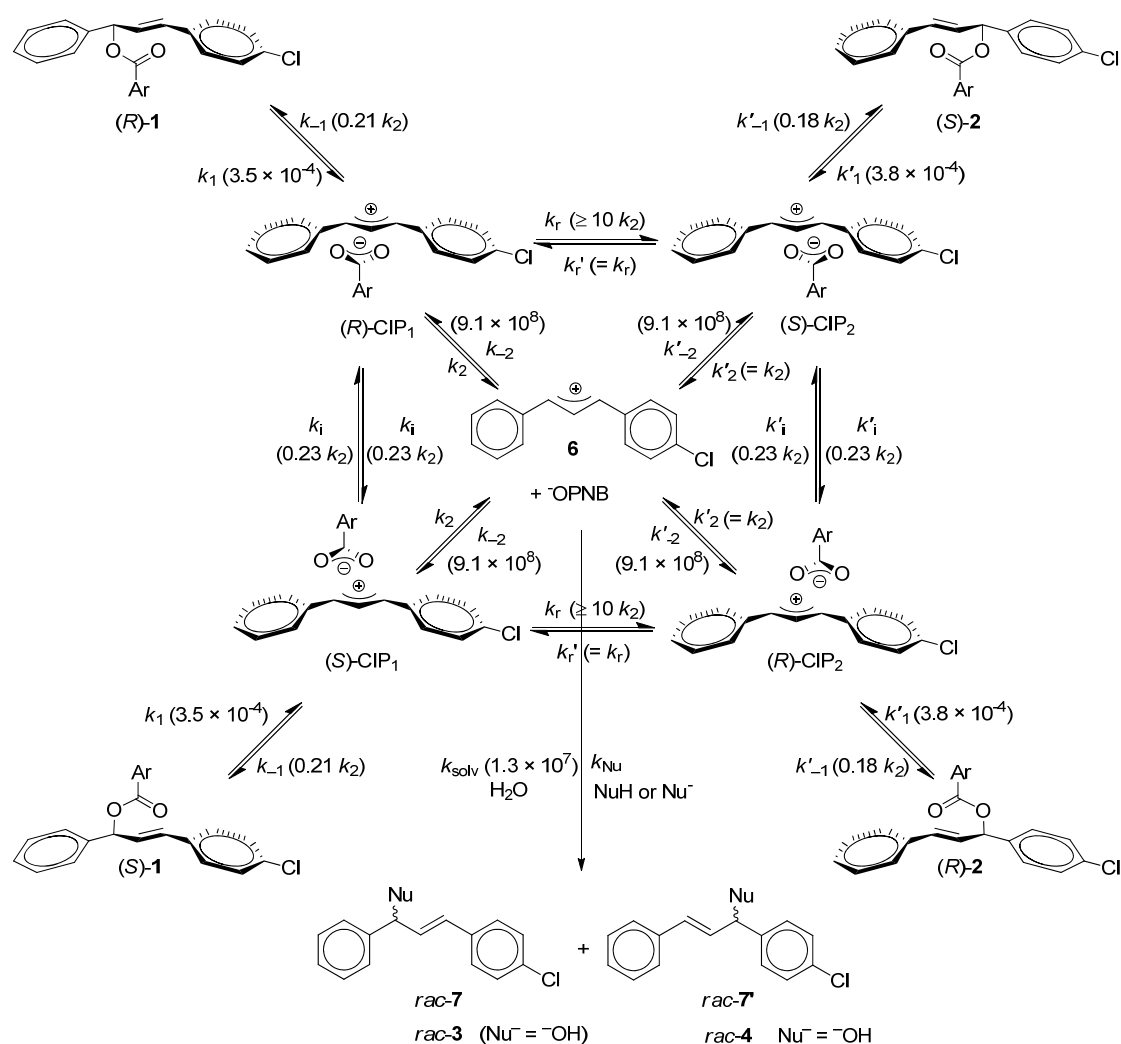
situation is observed when (*S*)-**2** is used as a substrate, where internal return favors the formation of (*R*)-**1** (suprafacial migration product). Table 3 shows that the ratio [(*S*)-**1**]/[(*R*)-**2**] obtained by solvolysis of either (*R*)-**1** or (*S*)-**2** is the same within experimental accuracy, indicating common intermediates from both precursors. This observation definitely excludes that the rearrangements (*R*)-**1**  $\rightarrow$  (*S*)-**1** and (*S*)-**2**  $\rightarrow$  (*R*)-**2** are preferred over the rearrangements (*R*)-**1**  $\rightarrow$  (*R*)-**2** and (*S*)-**2**  $\rightarrow$  (*S*)-**1**, respectively. In other words, when the leaving group migrates to the other face of the allyl cation, it has no preference for the carbon from which it departs. The observation that the ratio [(*S*)-**1**]/[(*R*)-**2**] is comparable to the ratio of the hydrolysis products ([**3**]/[**4**] = 1.5), supports the suggestion that external return of <sup>-</sup>OPNB (the major source of (*S*)-**1** and (*R*)-**2** in the presence of Bu<sub>4</sub>NOPNB) and hydrolysis proceed via the same key intermediates, i.e., the free 1,3-diarylallyl cations **6**.

**Table 3.** The Ratios [(*S*)-**1**]/[(*R*)-**2**] at Certain Reaction Times During Solvolysis of (*R*)-**1** and (*S*)-**2** in the Presence of Various Additives (60% Aq Acetone, 25 °C).

substrate, additive	[( <i>S</i> )- <b>1</b> ]/[( <i>R</i> )- <b>2</b> ]	
	at 50 min	at 60 min
( <i>R</i> )- <b>1</b> , no additive	1.40	1.41
( <i>R</i> )- <b>1</b> , 4.8 mM Bu <sub>4</sub> NOPNB	1.28	1.29
( <i>R</i> )- <b>1</b> , 52.5 mM Bu <sub>4</sub> NOPNB	1.37	1.38
( <i>S</i> )- <b>2</b> , no additive	1.35	1.50

A summary of these observations is presented in Scheme 5. The ionization step ( $k_1$  starting from **1** or  $k'_1$  starting from **2**) provides contact ion pairs ((*R*)-CIP<sub>1</sub>, (*S*)-CIP<sub>1</sub>, (*R*)-CIP<sub>2</sub>, (*S*)-CIP<sub>2</sub>) which retain the stereochemical and regiochemical information of the covalent substrates, i.e., the 4-nitrobenzoate anion is still on the same face of the carbocationic plane, close to the carbon to which it was covalently bound in the starting material. While these unsymmetrical structures of the ion pairs are in agreement with previous suggestions by Goering<sup>54</sup> and Thibblin,<sup>55</sup> the distinction of four different ion pairs is in line with, but not inevitably required by our experimental data. Instead of assuming the rapidly equilibrating

1  
2  
3 pairs (*R*)-CIP<sub>1</sub>  $\rightleftharpoons$  (*S*)-CIP<sub>2</sub> and (*S*)-CIP<sub>1</sub>  $\rightleftharpoons$  (*R*)-CIP<sub>2</sub>, one might also assume that the same  
4  
5  
6 chiral ion pair is formed from (*R*)-**1** and (*S*)-**2**, which is enantiomeric to that generated from  
7  
8 (*S*)-**1** and (*R*)-**2**. The latter alternative is kinetically equivalent to the mechanism in Scheme 5  
9  
10 (four different CIPs) with  $k_r = k'_r = \infty$ . According to Scheme 5, the unsymmetrical contact ion  
11  
12 pairs can undergo recombination ( $k_{-1}$  and  $k'_{-1}$ ), suprafacial migration ( $k_r$  and  $k'_r$ ), inversion ( $k_i$ ,  
13  
14  $k'_i$ , the anion migrates to the opposite face of the allyl cation), and dissociation with formation  
15  
16 of free cations **6** ( $k_2$ ,  $k'_2$ ). The free cations can re-associate with 4-nitrobenzoate anions  
17  
18 regenerating the contact ion pairs with the second-order rate constants  $k_{-2}$  and  $k'_{-2}$ , or react  
19  
20 with other nucleophiles (represented in Scheme 5 with the effective first order rate constant  
21  
22  $k_{Nu}$  which corresponds to the sum of reactions with all external nucleophiles and water) to  
23  
24 produce the racemic products **3**, **4**, **7**, and **7'**. As the alcohols **3** and **4** are formed as racemates,  
25  
26 nucleophilic trapping of the chiral CIPs can be excluded in Scheme 5. Trapping of ion pairs  
27  
28 by external nucleophiles must be taken into account, however, when ion pairs of less  
29  
30 stabilized carbocations are involved.<sup>56</sup>  
31  
32  
33  
34  
35  
36  
37  
38  
39  
40  
41  
42  
43  
44  
45  
46  
47  
48  
49  
50  
51  
52  
53  
54  
55  
56  
57  
58  
59  
60

**Scheme 5.** Mechanism for the Solvolysis of Allyl 4-Nitrobenzoates **1** and **2**.<sup>a</sup>

<sup>a</sup> The rate constants shown in parentheses result from the fit described below. All first-order rate constants as well as the pseudo-first-order rate constant  $k_{\text{solv}}$  are given in  $\text{s}^{-1}$  and correspond to 60% aq acetone, 25 °C. Second-order rate constants  $k_{-2}$  and  $k'_{-2}$  are given in  $\text{M}^{-1} \text{s}^{-1}$ .

The gross rate constant of the diffusional encounter of **6** with  $^-\text{OPNB}$  ( $k_{\text{diff}}^{\text{OPNB}}$ ) is expressed by equation 1.

$$k_{\text{OPNB}}^{\text{diff}} = 2(k_{-2} + k'_{-2}) \quad (1)$$

The factor of 2 implies that the encounter of **6** with  $^-\text{OPNB}$  is split into two equal pathways leading to the enantiomeric ion pairs.



The interconversions depicted in Scheme 5 can be described by the rate laws in eq 2 to eq 10.

$$\frac{d[(R)-\mathbf{1}]}{dt} = -k_1[(R)-\mathbf{1}] + k_{-1}[(R)-\text{CIP}_1] \quad (2)$$

$$\frac{d[(S)-\mathbf{1}]}{dt} = -k_1[(S)-\mathbf{1}] + k_{-1}[(S)-\text{CIP}_1] \quad (3)$$

$$\frac{d[(R)-\mathbf{2}]}{dt} = -k'_1[(R)-\mathbf{2}] + k'_{-1}[(R)-\text{CIP}_2] \quad (4)$$

$$\frac{d[(S)-\mathbf{2}]}{dt} = -k'_1[(S)-\mathbf{2}] + k'_{-1}[(S)-\text{CIP}_2] \quad (5)$$

$$\frac{d[(R)-\text{CIP}_1]}{dt} = k_1[(R)-\mathbf{1}] + k'_r[(S)-\text{CIP}_2] + k_i[(S)-\text{CIP}_1] + k_{-2}[\mathbf{6}][^-\text{OPNB}] - (k_{-1} + k_r + k_i + k_2)[(R)-\text{CIP}_1] \quad (6)$$

$$\frac{d[(S)-\text{CIP}_1]}{dt} = k_1[(S)-\mathbf{1}] + k'_r[(R)-\text{CIP}_2] + k_i[(R)-\text{CIP}_1] + k_{-2}[\mathbf{6}][^-\text{OPNB}] - (k_{-1} + k_r + k_i + k_2)[(S)-\text{CIP}_1] \quad (7)$$

$$\frac{d[(R)-\text{CIP}_2]}{dt} = k'_1[(R)-\mathbf{2}] + k_r[(S)-\text{CIP}_1] + k'_i[(S)-\text{CIP}_2] + k'_{-2}[\mathbf{6}][^-\text{OPNB}] - (k'_{-1} + k'_r + k'_i + k'_2)[(R)-\text{CIP}_2] \quad (8)$$

$$\frac{d[(S)-\text{CIP}_2]}{dt} = k'_1[(S)-\mathbf{2}] + k_r[(R)-\text{CIP}_1] + k'_i[(R)-\text{CIP}_2] + k'_{-2}[\mathbf{6}][^-\text{OPNB}] - (k'_{-1} + k'_r + k'_i + k'_2)[(S)-\text{CIP}_2] \quad (9)$$

$$\frac{d[\mathbf{6}]}{dt} = k_2[(R)-\text{CIP}_1] + k_2[(S)-\text{CIP}_1] + k'_2[(R)-\text{CIP}_2] + k'_2[(S)-\text{CIP}_2] - (2k_{-2}[^-\text{OPNB}] + 2k'_{-2}[^-\text{OPNB}] + k_{\text{Nu}})[\mathbf{6}] \quad (10)$$

The solution of the system of linear ordinary differential equations 2 to 10 provides the calculated values for the time-dependent concentrations of (R)-**1**, (S)-**1**, (R)-**2**, and (S)-**2** for a given set of parameters ( $k_1$ ,  $k'_{-1}$ ,  $k_{-1}$ ,  $k'_1$ ,  $k_r$ ,  $k_i$ ,  $k'_r$ ,  $k'_i$ ,  $k_2$ ,  $k'_2$ ,  $k_{-2}[^-\text{OPNB}]$ ,  $k'_{-2}[^-\text{OPNB}]$ ,  $k_{\text{Nu}}$ ).<sup>57</sup> In order to determine the individual rate constants shown in Scheme 5, we have simulated the time-dependent concentrations of the four isomeric esters (R)-**1**, (S)-**1**, (R)-**2**, and (S)-**2** during the solvolysis in 60% aq acetone of:

- (R)-**1** (0.80 mM) in the presence of 70.8 mM NaN<sub>3</sub>, which provides reliable data for internal return because external return of <sup>-</sup>OPNB is almost completely suppressed ( $k_{-2}[^-\text{OPNB}] \ll k_{\text{Nu}} = k_{\text{N}_3}[\text{N}_3^-] + k_{\text{solv}}$ ).
- (S)-**2** (0.79 mM) in the presence of 76.6 mM NaN<sub>3</sub>.
- (R)-**1** (0.80 mM) in the presence of 4.8 mM Bu<sub>4</sub>NOPNB (to keep  $k_{-2}[^-\text{OPNB}]$  and  $k'_{-2}[^-\text{OPNB}]$  constant during the reaction, which provides the reliable data for external return).

The directly measured rate constant of the reaction of **6** with water in 60% aq acetone ( $k_{\text{solv}} = 1.34 \times 10^7 \text{ s}^{-1}$ ) and the second-order rate constant  $k_{\text{N3}}$  ( $6.1 \times 10^9 \text{ M}^{-1}\text{s}^{-1}$ ), which was derived from  $k_{\text{solv}}$  and the allyl azide/allyl alcohol ratio, were introduced as fixed quantities.

As the free energies of the ion pairs CIP<sub>1</sub> and CIP<sub>2</sub> are closely similar, the corresponding rate constants for diffusion and ion pair reorganization were set equal, i.e.,  $k'_2 = k_2$ ,  $k'_{-2} = k_{-2}$ ,  $k'_r = k_r$ , and  $k'_i = k_i$ . The small errors introduced by these assumptions are compensated by the relative magnitudes of the recombination rate constants  $k'_{-1}/k_{-1}$ .

Minimization of the sum of squared deviations (SSD) between calculated and experimental time-dependent concentrations of all isomeric esters (*R,S*)-**1** and (*R,S*)-**2** yielded the values of the rate constants which fit the experiments most correctly.

As shown in Table SN1 (page S67) of the Supporting Information  $k_2 = k'_2$  was arbitrarily set at values between  $10^8$  and  $10^{11} \text{ s}^{-1}$ , while the remaining parameters were optimized. The last column of the Table SN1 shows that equally good fits between calculated and experimental concentrations were obtained for the different values of  $k_2 = k'_2$ . While  $k_1$ ,  $k'_1$ ,  $k_{-2}$ , and  $k'_{-2}$  were found to be independent ( $\pm 4\%$ ) of the choice of  $k_2$  in the specified range,  $k_{-1}$ ,  $k'_{-1}$ , and  $k_i = k'_i$  were found to be directly proportional to  $k_2$  (Figures SN1 to SN8 of the Supporting Information), which allowed us to express these rate constants as multiples of  $k_2$  in Scheme 5. For a fixed value of  $k_2 = k'_2 = 2 \times 10^{10} \text{ s}^{-1}$ , comparable SSDs were obtained for different values of  $k_r$  as long as they were greater than  $10k_2$ , and the values of  $k_{-1}$ ,  $k'_{-1}$ ,  $k_i = k'_i$  changed insignificantly ( $< 7\%$ ) when  $k_r = k'_r$  was varied from  $10k_2$  to  $500k_2$ , (Figures SN9 to SN15 of the Supporting Information). As a consequence, each value of  $k_2$  entails certain values ( $\pm 7\%$ ) of  $k_{-1}$ ,  $k'_{-1}$ ,  $k_i = k'_i$  and lower limits for  $k_r = k'_r$ . The same results were obtained when the steady state approximation was applied to (*R*)-CIP<sub>1</sub>, (*S*)-CIP<sub>1</sub>, (*R*)-CIP<sub>2</sub>, (*S*)-CIP<sub>2</sub>, and **6** (Figures SN1a to SN8a of the Supporting Information). The resulting absolute and relative rate constants are presented in Scheme 5.

The good agreement between calculated and experimental time-dependent concentrations (Figure 7 and Figures SN18 to SN19 of the Supporting Information) demonstrates that the solvolyses of **1** and **2** can adequately be described by the mechanism presented in Scheme 5.

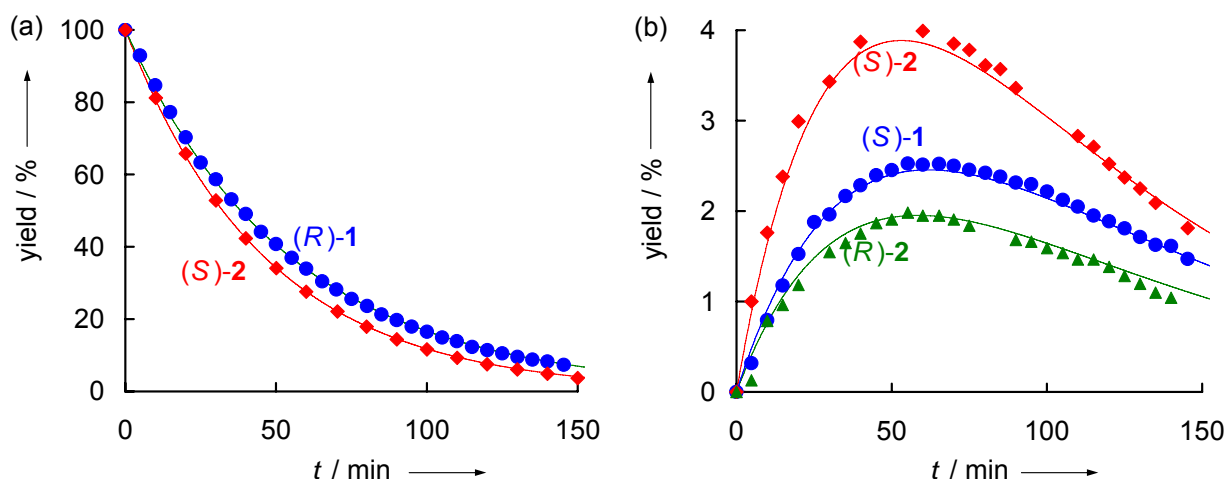


**Figure 7.** Calculated (solid lines) and experimental time-dependent concentrations of (a) (*R*)-**1** (0.80 mM) and (*S*)-**2** (0.79 mM) during their solvolysis in 60% aq acetone in the presence of 4.8 mM Bu<sub>4</sub>NOPNB and 76.6 mM NaN<sub>3</sub>, respectively; and (b) of (*S*)-**1**, (*S*)-**2**, and (*R*)-**2** during solvolysis of (*R*)-**1** (0.80 mM) in 60% aq acetone in the presence of 4.8 mM Bu<sub>4</sub>NOPNB, 25 °C.

According to Scheme 5, the slowest step of the solvolysis is the initial ionization leading to the CIPs ( $k_1 = 3.5 \times 10^{-4} \text{ s}^{-1}$ ,  $k'_1 = 3.8 \times 10^{-4} \text{ s}^{-1}$ ). Suprafacial migration of the 4-nitrobenzoate anion ( $k_r = k'_r > 10k_2$ ) is the most likely transformation of the CIP, followed by dissociation ( $k_2 = k'_2$ ) and, finally, inversion ( $k_i = k'_i = 0.23k_2$ ) and ion pair collapse ( $k_{-1} = 0.21k_2$ ,  $k'_{-1} = 0.18k_2$ ), which have almost equal rates. This sequence explains the partial stereospecificity of internal return, i.e., the fact that (*S*)-**2** is the major product among the rearranged esters during solvolysis of (*R*)-**1** and vice versa.

Because of the availability of the directly measured rate constant  $k_{\text{sol}}$  for the reaction of **6** with water (in aq acetone), our experiments provide an accurate value for the diffusional

process generating ion pairs from the free ions **6** ( $k_{-2} = k'_{-2}$ ). On the other hand, the rate constants for the diffusional separation of the ion pairs ( $k_2 = k'_2$ ) cannot be derived directly from the experimental data. As values of  $10^8 < k_2/s^{-1} < 10^{11}$  give equally good fits, the value of

$k_2 \approx 1.6 \times 10^{10} \text{ s}^{-1}$ , which was proposed by Richard and Jencks<sup>35</sup> and is mostly used in the literature, appears to be a good choice also for this system.

From the value of  $k_{-2} = k'_{-2} = 9.1 \times 10^8 \text{ M}^{-1}\text{s}^{-1}$  one can calculate the second-order rate constant of diffusional migration of 4-nitrobenzoate anion to the free cation **6** using eq 1 ( $k_{\text{diff}}^{\text{OPNB}} = 4k_{-2} = 3.6 \times 10^9 \text{ M}^{-1}\text{s}^{-1}$ ), which is similar to the value of  $1.5 \times 10^9 \text{ M}^{-1}\text{s}^{-1}$  reported by Tsuji, Richard, and co-workers for the diffusion of carboxylate anions to the 1-(4-methylphenyl)ethyl cation in 50% v/v TFE-water mixture.<sup>36a</sup>

Earlier analyses, which were based on titrimetric, polarimetric, and  $^{18}\text{O}$ -exchange rate constants, left the question open whether solvolysis and internal return are two independent processes involving different types of ion pairs.<sup>33</sup> As simulations based on Scheme 5 accurately describe the distribution of the products generated by internal and external return, it is now clear that solvolysis and internal return can be explained by the same intermediates.

## A Comprehensive View on Solvolyses of Allyl Carboxylates.

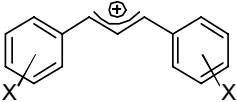
The kinetic and stereochemical investigations of the solvolyses of the enantiopure allyl carboxylates (*R*)-**1** and (*S*)-**2** provided detailed information on relative and absolute rates of the individual steps for the system described in Scheme 5. Can one use these results to derive a general scheme of solvolyses of allyl carboxylates?

In previous work,<sup>44</sup> we have determined the electrophilicity parameters  $E$  of the symmetrical 1,3-diarylallyl cations X-**10**, which are listed in Table 4. According to equation 11, the electrophilicity parameters  $E$  can be combined with the solvent-dependent nucleophile-specific parameters  $N$  and  $s_N$  to calculate second-order rate constants for the reactions of

carbocations with neutral and anionic nucleophiles<sup>39</sup> as well as the first-order rate constants for the reactions of carbocations with the solvents.<sup>38</sup>

$$\log k (20\text{ }^{\circ}\text{C}) = s_{\text{N}} (E + N) \quad (11)$$

**Table 4.** Symmetrical 1,3-Diarylallyl Cations **X-10** and Their Electrophilicity Parameters  $E$ .<sup>44</sup>



**X - 10**

<b>X-10</b>	<b>X</b>	<b><math>E</math></b>
<b>F<sub>2</sub>-10</b>	<i>m,m</i> -F <sub>2</sub>	6.11
<b>F-10</b>	<i>m</i> -F	4.15
<b>Br-10</b>	<i>p</i> -Br	2.85
<b>Cl-10</b>	<i>p</i> -Cl	2.69
<b>H-10</b>	H	2.70
<b>Me-10</b>	<i>p</i> -Me	1.23
<b>MeO-10</b>	<i>p</i> -MeO	-1.45
<b>Me<sub>2</sub>N-10</b>	<i>p</i> -Me <sub>2</sub> N	-7.50

As the 1,3-diphenylallyl cation **H-10** and its dichloro-substituted analogue **Cl-10** have almost the same values of  $E$ , the same electrophilicity ( $E = 2.70$ ) can also be assumed for the monochlorinated system **6**.

**Rates of Reactions of the Allyl Cations 10 with Aqueous Acetone.** Investigations of the nucleophilic reactivities of solvents have shown that acetonitrile/water mixtures with 20% to 90% content of water (v/v) react with equal rates with benzhydrylium ions,<sup>38</sup> in accordance with earlier reports by McClelland.<sup>58</sup> The same relationship seems to hold also for acetone/water mixtures, as 90% ( $N = 5.70$ ,  $s_{\text{N}} = 0.85$ ) and 80% aq acetone ( $N = 5.77$ ,  $s_{\text{N}} = 0.87$ ) were reported to react with similar rates.<sup>59</sup> Accordingly, the first-order rate constant for the reaction of **6** ( $E = 2.70$ ) with 80% aq acetone calculated by eq 11 ( $2.3 \times 10^7\text{ s}^{-1}$ ) agrees well with the directly measured rate constant for the reaction of **6** with 60% aqueous acetone

( $1.34 \times 10^7 \text{ s}^{-1}$ , see above). Equation 11 can thus be employed also to calculate the rate constants for the reactions of **10** with aqueous acetone.

It should be noted that the agreement within a factor of 2 between the calculated and experimental rate constant for the reaction of **6** with aqueous acetone cannot a priori be expected, because deviations up to factors of 10–100 have to be tolerated for predictions of absolute rate constants by equation 11, which covers a reactivity range of 40 orders of magnitude with only three parameters.<sup>41,60</sup> On the other hand, equation 11 allows one to predict relative reactivities within reaction series, e.g., the relative reaction rates of X-**10**,<sup>44</sup> with an accuracy better than factor of 2.<sup>43,60</sup>

**Rates of Reactions of the Allyl Cations 10 with the 4-Nitrobenzoate Anion.** In order to apply equation 11, let us first derive the nucleophilicity parameter  $N$  for the 4-nitrobenzoate anion ( $^-\text{OPNB}$ ) in 60% aq acetone. At low concentrations of the substrates, as they are usually employed in solvolysis experiments, the concentration of ion pairs (corresponding to encounter-complexes in ion-molecule or molecule-molecule reactions) is small compared with the concentrations of the non-paired reactants, and the rate constant for the recombination of **6** with  $^-\text{OPNB}$  to the covalent products **1** and **2** is given by eq 12, which expresses the rate constants for ion recombination  $k_{\text{rec}}$  by multiplying the constant of the diffusional association ( $k_{-2}$ ) with the partitioning factor (forward reaction,  $k_{-1}$ , divided by the sum of forward and backward reactions,  $k_{-1} + k_2$ ) and the corresponding term for attack at the other allyl terminus.

$$k_{\text{rec}} = 2k_{-2} \frac{k_{-1}}{k_{-1} + k_2} + 2k'_{-2} \frac{k'_{-1}}{k'_{-1} + k'_2} \quad (12)$$

Substitution of  $k_{-1}$ ,  $k'_{-1}$ ,  $k_{-2}$ , and  $k'_{-2}$  by the absolute values or multiples of  $k_2$  presented in Scheme 5 yields  $k_{\text{rec}} = 5.91 \times 10^8 \text{ M}^{-1}\text{s}^{-1}$  for the reaction of **6** with  $^-\text{OPNB}$  in 60% aq acetone.

As  $k_{\text{rec}} > 10^8 \text{ M}^{-1}\text{s}^{-1}$ , i.e., beyond the range which is covered by equation 11,  $k_{\text{rec}}$  cannot be directly substituted in equation 11 to calculate  $N$ .

For the sake of simplicity, let us adjust equation 12 to symmetrically substituted allyl cations, e.g., **10**. For  $k'_{-1} = k_{-1}$ ,  $k'_2 = k_2$ , and  $k'_{-2} = k_{-2}$  equation 12 simplifies to equation 13.

$$k_{\text{rec}} = 4k_{-2} \frac{k_{-1}}{k_{-1} + k_2} \quad (13)$$

In activation-controlled reactions of **10** with  $^-\text{OPNB}$ , diffusional separation is much faster than the formation of the covalent esters ( $k_2 \gg k_{-1}$ ), which reduces equation 13 to equation 14.

$$k_{\text{rec}} = 4k_{-2} \frac{k_{-1}}{k_2} \quad (14)$$

It should be noted that equations 13 and 14 correspond to the typical treatment of diffusion- and activation-controlled reactions described in standard textbooks.<sup>61</sup>

In order to apply the linear free energy relationship (equation 11) also to reactions which are affected by diffusion rates ( $k > 10^8 \text{ M}^{-1}\text{s}^{-1}$ ), one has to multiply the rate constants calculated by equation 11 (which refer to activation-controlled reactions) with the correction factor  $f$  (eq 15) which is obtained by dividing equation 13 by equation 14.

$$f = \frac{k_2}{k_2 + k_{-1}} \quad (15)$$

For  $k_{-1} = 0.193k_2$  (average of  $k_{-1}$  and  $k'_{-1}$ , Scheme 5),<sup>62</sup> one obtains  $f = 0.84$ . Division of the experimental rate constant for the reaction of **6** with  $^-\text{OPNB}$  ( $5.91 \times 10^8 \text{ M}^{-1}\text{s}^{-1}$ ) by  $f = 0.84$  leads to  $7.04 \times 10^8 \text{ M}^{-1}\text{s}^{-1}$ , which can be substituted into eq 11 to derive  $N(^-\text{OPNB}) = 9.94$ , using  $E(\text{6}) = 2.70$  and  $s_N = 0.7$ , the typical sensitivity parameter for carboxylate anions in aqueous and polar organic solvents.<sup>37</sup> The  $N$  and  $s_N$  parameters for  $^-\text{OPNB}$  can now be combined with the  $E$  values of X-**10** (Table 4) to calculate the rate constants for the reactions of X-**10** with 4-nitrobenzoate anion in 60% aq acetone.

**Probabilities of Internal and External Return.** Internal return occurs, when the value of  $k_{-1}$  is comparable to or greater than the rate constant of diffusional separation of the ion pairs ( $k_2$ ). Its probability is given by equation 16.

$$p_{\text{IR}} = \frac{k_{-1}}{k_{-1} + k_2} 100\% \quad (16)$$

From equations 14 and 11 one gets the relationship (17), which allows expressing  $k_{-1}$  as a function of  $E$  (eq 18).

$$s_N(E + N) = \log 4k_{-2} + \log \frac{k_{-1}}{k_2} \quad (17)$$

$$\log k_{-1} = s_N(E + N) + \log k_2 - \log 4k_{-2} \quad (18)$$

For the sake of simplicity, let us assume that the linear dependence of  $\log k_{-1}/k_2$  on  $E$ , which is expressed by eqs 17 and 18, also holds for reactions beyond the activation-controlled region (i.e., for reactions where  $k_{-1}$  is comparable to  $k_2$ ).<sup>63</sup> One then arrives at Figure 8 which illustrates the increase of the rate of ion pair collapse ( $k_{-1}$ , from eq 18) with increasing electrophilicity  $E$  of the allyl cations X-**10** in comparison with the rate constant for diffusional separation ( $k_2$ ), for which Richard's<sup>35</sup> estimate of  $1.6 \times 10^{10} \text{ s}^{-1}$  is used.

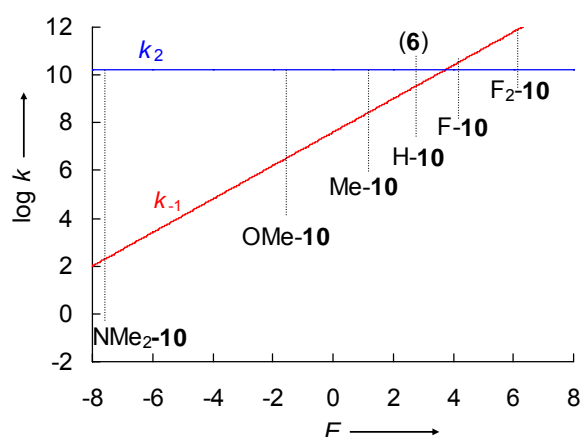


**Figure 8.** Relationship between internal return ( $k_{-1}$  vs  $k_2$ ) and the electrophilicities  $E$  of the carbenium ions **10** during solvolyses of 1,3-diarylallyl 4-nitrobenzoates **10**-OPNB in 60% aq acetone.



One can see that the lines cross at  $E \approx 4$ , i.e., internal return becomes dominant for the highly electrophilic carbocations on the right of Figure 8. The  $k_{-1}$  graph is only slightly below the  $k_2$  line for cation **6**, which reflects the participation of internal return expressed by the  $k_{-1}/k_2$  ratio in Scheme 5. It should be emphasized that this analysis does not depend on the exact magnitude of  $k_2$ . According to eq 18, variation of  $k_2$  would also affect  $k_{-1}$ , and shift the crossing point of the two correlation lines in Figure 8 vertically, not horizontally, i.e., the nature of the carbocation ( $E$  value) where these lines cross would not be affected. The  $E$  value of the crossing point would move slightly, however, when the linear dependence of  $\log k_{-1}/k_2$  on  $E$  is not followed accurately in the diffusion-controlled range, as assumed above.

The probability of external return is given by the relative rates of the reactions of the free 1,3-diarylallyl cation **10** with 4-nitrobenzoate anion ( $k_{\text{rec}}[\text{OPNB}]^-$ ) and the solvent ( $k_{\text{solv}}$ , as described by equation 19.

$$p_{\text{ER}} = \frac{k_{\text{rec}}[\text{OPNB}]^-}{k_{\text{rec}}[\text{OPNB}]^- + k_{\text{solv}}} 100\% \quad (19)$$

Figure 9 compares the pseudo-first-order rate constants for the reactions of the allyl cations **10** with the 4-nitrobenzoate anion in 60% aq acetone (at  $[\text{OPNB}]^- = 5 \text{ mM}$ ) and with the solvent calculated by equation 11. The curved part of the  $k_{\text{rec}}$  graph, which describes the approach to the diffusion limit, was obtained by multiplication of the rate constants calculated by equation 11 with the correction factor  $f$  of equation 15. The curvature of the correlation line for the solvent, which is irrelevant for the following discussion, is estimated from preliminary results in our group.<sup>64</sup>

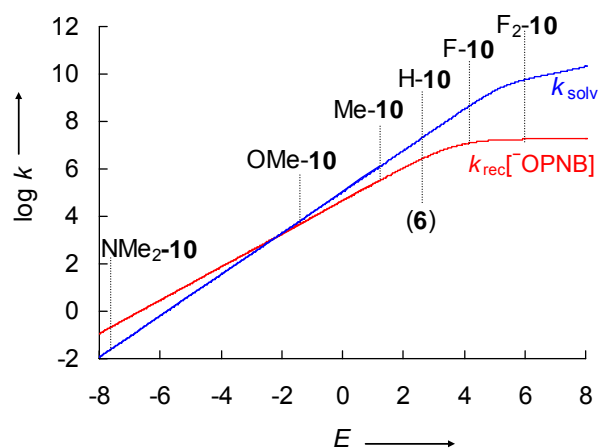


**Figure 9.** Relationship between external return ( $k_{\text{rec}}$  vs  $k_{\text{solv}}$ ) and the electrophilicities  $E$  of the carbenium ions **10** during solvolyses of 1,3-diarylallyl 4-nitrobenzoates **10**-OPNB in 60% aq acetone for  $[\text{}^-\text{OPNB}] = 5 \text{ mM}$  (25 °C).

As previously shown for solvolyses of benzhydryl and trityl derivatives,<sup>41</sup> external (common ion) return is faster than the reaction with solvent for highly stabilized carbocations, while highly reactive carbocations are so rapidly trapped by the solvent that the leaving group  $\text{}^-\text{OPNB}$  does not have a chance to compete because of its low concentration, even when the ion combination is diffusion-controlled.

The probabilities of internal return  $p_{\text{IR}}$  and external return  $p_{\text{ER}}$  can be calculated by eqs 16 and 19 and are plotted against  $E$  in Figure 10.<sup>65</sup>

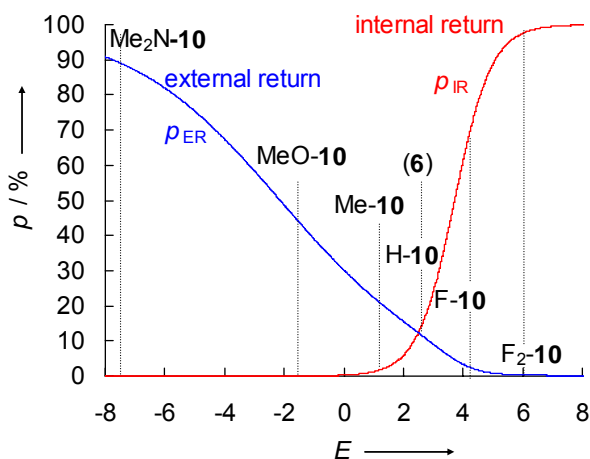


**Figure 10.** Dependencies of  $p_{\text{IR}}$  and  $p_{\text{ER}}$  for solvolyses of 1,3-diaryllallyl 4-nitrobenzoates **10**-OPNB in 60% aq acetone (25 °C) on the  $E$  values of the cations **10** for  $[\text{OPNB}] = 5 \text{ mM}$ .

According to Figure 10, solvolyses of 1,3-diaryllallyl 4-nitrobenzoates in 60% aq acetone (at  $[\text{OPNB}] = 5 \text{ mM}$ ) which proceed via highly stabilized carbenium ions ( $E < 0$ , e.g., **Me<sub>2</sub>N-10** or **MeO-10**) do not occur with internal return because their diffusional escape from the ion pair cage is faster than ion pair collapse; allylic rearrangements of such systems should proceed completely non-stereospecific. Both external and internal return can be expected for the solvolyses of 4-nitrobenzoates derived from carbenium ions with  $1 < E < 5$ . While the extent of external and internal return is comparable for **H-10**-OPNB or **6**-OPNB ( $p_{\text{IR}} = 16\%$ ,  $p_{\text{ER}} = 11\%$ ), solvolysis via better stabilized allyl cations ( $E < 2.7$ ) should give more external and those via less stabilized carbocations should give more internal return. Thus, 4-nitrobenzoates derived from carbenium ions with  $E > 6$  (e.g., **F<sub>2</sub>-10**-OPNB), should solvolyze without external and with a large degree of internal return, i.e., allylic rearrangements of unsymmetrical systems involving carbocations of such high electrophilicities can be expected to be highly stereospecific.

The far right part of Figure 10 has to be seen with some caveat, however, because it is based on the premise that solvent and 4-nitrobenzoate anions only attack at free cations and not at ion pairs, as demonstrated for the solvolysis of **6**-OPNB in this work. It is feasible, however,

that in the case of highly electrophilic carbenium ions, direct solvent capture of the CIPs will occur, resulting in a decrease of the probability of internal return.

The scheme presented for 1,3-diarylallyl 4-nitrobenzoates in 60% aq acetone in Figure 10, i.e., increase of  $p_{\text{IR}}$  and decrease of  $p_{\text{ER}}$  with increasing electrophilicity  $E$ , should analogously hold for other leaving groups and solvents, though the positions of the curves and their shapes will change. Figure 11 illustrates the calculated curves for external and internal return for  $\text{Br}^-$  ( $N = 13.80$ ,  $s_N = 0.60$ ), a significantly stronger nucleophile<sup>37,38</sup> (though a weaker Lewis base) than  $^-\text{OPNB}$ , in 50% aq acetonitrile ( $N = 5.05$ ,  $s_N = 0.89$ ), a solvent of similar nucleophilicity as aqueous acetone.

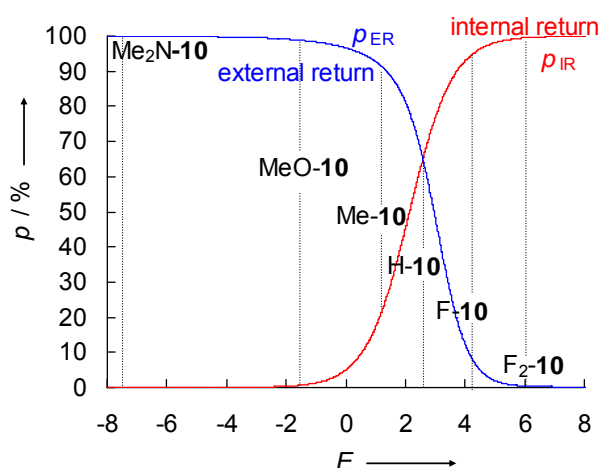


**Figure 11.** Estimated dependencies of  $p_{\text{IR}}$  and  $p_{\text{ER}}$  for solvolyses of 1,3-diarylallyl bromides **10**-Br in 50% aq acetonitrile (25 °C) on the  $E$  values of the cations **10** for  $[\text{Br}^-] = 5 \text{ mM}$ .

One can see that the graph for internal return is similar to that in Figure 10, but shifted to less electrophilic carbocations, implying that internal return plays a greater role because of the higher nucleophilicity of  $\text{Br}^-$ . The graph for external return is almost the same in the right part of Figures 10 and 11 because both  $\text{Br}^-$  and  $^-\text{OPNB}$  undergo diffusion-controlled reactions with carbocations in this range and have comparable chances to compete with the nucleophilic attack by water. Moving to the left, i.e., to less electrophilic carbocations, leads to a much faster increase of external return in Figure 11, because now the better nucleophile  $\text{Br}^-$  can

more efficiently compete with water than the weaker nucleophile  $^-OPNB$ . It should be noted, however, that the far left part of this graph is hypothetical. Though a fast reaction of  $Me_2N-10$  with  $Br^-$  will occur, the reverse reaction can be expected to be even faster, with the result that  $Me_2N-10^+Br^-$  will be predominantly ionic in 50% aqueous acetonitrile.

Decrease of the water content in acetone/water and acetonitrile/water mixtures is known to increase the nucleophilicity parameters  $N$  of the commonly used anionic leaving groups,<sup>39,66</sup> resulting in an increase of  $k_{-1}$  according to equation 18 and consequently lead to an increase in  $p_{IR}$  (eq 16). As an increase of  $N$  will also increase  $k_{rec}$  (eq 11) and consequently  $p_{ER}$  (eq 19; the small decrease of  $k_{solv}$  in solvents with a lower content of water will shift  $p_{ER}$  in the same direction), also the probability of external return will grow. In line with this analysis, Figures 3 and 4 show an increase of the yields of all isomerization products ((*S*)-**1**, (*R*)-**2**, and (*S*)-**2**) generated during the solvolysis of (*R*)-**1** when the solvent was changed from 60% to 80% and 90% aq acetone. In the same way, one can rationalize Goering's observations that the ratio  $k_a/k_t$  (polarimetric rate constant/titrimetric rate constant) for the solvolyses of *cis*-5-methylcyclohex-2-enyl 2-carboxybenzoate,<sup>26</sup> *trans*-5-methylcyclohex-2-enyl 4-nitrobenzoate,<sup>27b</sup> and 1,3-dimethylallyl 4-nitrobenzoate<sup>67</sup> in aqueous acetone generally increased with decreasing water content because of the increasing nucleophilicities of the carboxylate ions. The enhancement of internal return with increasing electrophilicities of the carbenium ions is also in agreement with conclusions of Yabe and Kochi, which were derived from the rates of the recombinations of anthracenylium radical cation-trinitromethide ion pairs generated by laser-flash-induced electron transfer in the anthracene-tetranitromethane complexes.<sup>32</sup>

## Conclusions

The time-dependent concentrations of the four isomeric esters (*R,S*)-**1** and (*R,S*)-**2** and the four isomeric alcohols (*R,S*)-**3** and (*R,S*)-**4** measured during the hydrolysis of enantiopure (*R*)-**1** and (*S*)-**2** in aqueous acetone in the presence and absence of external nucleophiles were combined with the measured rate constant for the reaction of the laser-flash photolytically generated allyl cation **6** with water in aqueous acetone in order to develop a complete mechanistic scheme for this solvolysis cascade. As depicted in Scheme 5, the slowest step is the initial ionization leading to the CIPs ( $k_1 = 3.5 \times 10^{-4} \text{ s}^{-1}$ ,  $k'_1 = 3.8 \times 10^{-4} \text{ s}^{-1}$ ). Suprafacial migration of the 4-nitrobenzoate anion ( $k_r = k'_r > 10k_2$ ) is the most likely transformation of the CIP, followed by dissociation ( $k_2 = k'_2$ ) and, finally, inversion ( $k_i = k'_i = 0.23k_2$ ) and ion pair collapse ( $k_{-1} = 0.21k_2$ ,  $k'_{-1} = 0.18k_2$ ). This sequence explains the partial stereospecificity of internal return, i.e., the fact that (*S*)-**2** is the major product among the rearranged esters during solvolysis of (*R*)-**1** and vice versa. As simulations based on Scheme 5 accurately describe the distribution of the products generated by internal and external return, it is now clear that solvolysis and internal return can be explained by the same intermediates.

The results of this work were combined with previously determined electrophilicity parameters  $E$  for 1,3-diarylallyl cations X-**10** to analyze the role of internal and external return in solvolyses of 1,3-diarylallyl 4-nitrobenzoates. While the parent 1,3-diphenylallyl 4-nitrobenzoate ( $E = 2.7$ ) is predicted to solvolyze with 16% internal and 11% external return,<sup>65</sup> the contribution of external return increases, and the contribution of internal return decreases with increasing stabilization (decreasing electrophilicity  $E$ ) of the allyl cations (Figure 10).

The correlation equation 11, which calculates rate constants of the reactions of carbocations with nucleophiles from the electrophile-specific parameter  $E$  and the nucleophile-specific parameters  $N$  and  $s_N$ , can be used to estimate the role of internal and external return also for other substrates.

## Experimental

Acetone (99.8%), hexane, and isopropanol (HPLC grade) were used as received. Double distilled water (impedance 18.2  $\Omega$ ) was obtained from a water purification system. Tetrabutylammonium chloride and sodium azide were purchased and used without further purification. Tetrabutylammonium 4-nitrobenzoate and tetrabutylammonium benzoate were synthesized by using the procedure described in ref 37. Sharpless kinetic resolution followed by acylation was used for synthesis of optically active **1** and **2**. The absolute configuration of (*R*)-**1** was confirmed by X-ray diffraction analysis.<sup>68</sup> The precursors for laser-flash measurements, **8** and **9**, were generated in situ from the mixture of 1-(4-chlorophenyl)-3-phenylallyl and 3-(4-chlorophenyl)-1-phenylallyl chlorides (**11**) synthesized from **3** using the procedure from ref 69 and 1,2,3,4,5,6-hexahydro-1,3a,6,8-tetraazaphenalene (**12**) obtained as reported by David and coworkers.<sup>70</sup> Detailed descriptions of HPLC experiments, laser-flash kinetic measurements, and NMR product studies as well as all synthetic procedures can be found in the Supporting Information.

**Acknowledgements.** We thank the Deutsche Forschungsgemeinschaft (Ma 673/22-1) for financial support. We are grateful to Anna Antipova, Ian Dunn, and Dr. Armin R. Ofial for their help during preparation of this manuscript as well as to Tobias A. Nigst for providing a sample of **12** and to Johannes Ammer for helpful discussions. We also thank Prof. Dr. Paul Knochel for his valuable suggestions concerning synthesis of optically active **3** and **4**.

**Supporting Information Available:** Details of the kinetic experiments, evaluation of the microscopic rate constants, synthetic procedures and product studies, as well as NBO calculation for cation **6**. This material is available free of charge via the Internet at <http://pubs.acs.org>.

## References

1. Kotke, M.; Schreiner, P. R. (Thio)urea organocatalysts. In *Hydrogen Bonding in Organic Synthesis*; Pihko, P. M., Ed.; Wiley, Weinheim, 2009.
2. Phipps, R. J.; Hamilton, G. L.; Toste, F. D. *Nat. Chem.* **2012**, *4*, 603–614.
3. Dolling, U.-H.; Davis, P.; Grabowski, E. J. J. *J. Am. Chem. Soc.* **1984**, *106*, 446–447.
4. (a) Ooi, T.; Maruoka, K. *Angew. Chem., Int. Ed.* **2007**, *46*, 4222–4266. (b) *Asymmetric Phase Transfer Catalysis*; Maruoka, K., Ed.; Wiley, Weinheim, 2008.
5. For reviews on use of chiral Brønsted acids see for instance: (a) Akiyama, T. *Chem Rev.* **2007**, *107*, 5744–5758. (b) Rueping, M.; Nachtsheim, B. J.; Ieawsuwan, W.; Atodiresei, I. *Angew. Chem., Int. Ed.*, **2011**, *50*, 6706–6720.
6. (a) Nakashima, D.; Yamamoto, H. *J. Am. Chem. Soc.* **2006**, *128*, 9626–9627. (b) Jiao, P.; Nakashima, D.; Yamamoto, H. *Angew. Chem., Int. Ed.* **2008**, *47*, 2411–2413.
7. (a) Rueping, M.; Ieawsuwan, W.; Antonchick, A. P.; Nachtsheim, B. J. *Angew. Chem., Int. Ed.* **2007**, *46*, 2097–2100. (b) Müller, S.; List, B. *Angew. Chem., Int. Ed.* **2009**, *48*, 9975–9978.
8. Rueping, M.; Nachtsheim, B. J.; Moreth, S. A.; Bolte, M. *Angew. Chem., Int. Ed.* **2008**, *47*, 593–596.
9. Rueping, M.; Uria, U.; Lin, M.-Y.; Atodiresei, I. *J. Am. Chem. Soc.* **2011**, *133*, 3732–3735.
10. Hoffmann, S.; Seayad, A. M.; List, B. *Angew. Chem., Int. Ed.* **2005**, *44*, 7424–7427.
11. Rueping, M.; Theissmann, T.; Kuenkel, A.; Koenigs, R. M. *Angew. Chem., Int. Ed.* **2008**, *47*, 6798–6801.
12. Fleischmann, M.; Drettwan, D.; Sugiono, E.; Rueping, M.; Gschwind, R. M. *Angew. Chem. Int. Ed.* **2011**, *50*, 6364–6369.
13. (a) Ratjen, L.; Müller, S.; List, B. *Nachr. Chem.* **2010**, *58*, 640–646. (b) Mahlau, M.; List, B. *Isr. J. Chem.* **2012**, *52*, 630–638.



14. See, for instance: (a) Mayer, S.; List, B. *Angew. Chem., Int. Ed.* **2006**, *45*, 4193–4195. (b) Martin, N. J. A.; List, B. *J. Am. Chem. Soc.* **2006**, *128*, 13368–13369 (c) Wang, X.; List, B. *Angew. Chem., Int. Ed.* **2008**, *47*, 1119–1122.
15. (a) Llewellyn, D. B.; Adamson, D.; Arndtsen, B. A. *Org. Lett.* **2000**, *2*, 4165–4168. (b) Hamilton, G. L.; Kang, E. J.; Mba, M.; Toste, F. D. *Science* **2007**, *317*, 496–499. (c) LaLonde, R. L.; Wang, Z. J.; Mba, M.; Lackner, A. D.; Toste, F. D. *Angew. Chem., Int. Ed.* **2010**, *49*, 598–601. (d) Rauniyar, V.; Wang, Z. J.; Burks, H. E.; Toste, F. D. *J. Am. Chem. Soc.* **2011**, *133*, 8486–8489. (e) Liao, S.; List, B. *Angew. Chem., Int. Ed.* **2010**, *49*, 628–631.
- It should be noted that in some cases the chiral phosphate may act as ligand and not as counterion for the cationic metal complex. Examples of transformations, where phosphate ions were shown to act as ligands are, for instance: (f) Mukherjee, S.; List, B. *J. Am. Chem. Soc.* **2007**, *129*, 11336–11337. (g) Jiang, G; Halder, R; Fang, Y.; List, B. *Angew. Chem., Int. Ed.* **2011**, *50*, 9752–9755.
16. Ohmatsu, K.; Ito, M.; Kunieda, K.; Ooi, T. *Nat. Chem.* **2012**, *4*, 473–477.
17. Macchioni, A. *Chem. Rev.* **2005**, *105*, 2039–2074, and references therein.
18. (a) Raheem, I. T.; Thiara, P. S.; Peterson, E. A.; Jacobsen, E. N. *J. Am. Chem. Soc.* **2007**, *129*, 13404–13405. (b) Knowles, R. R.; Lin, S.; Jacobsen, E. N. *J. Am. Chem. Soc.* **2010**, *132*, 5030–5032. (c) Brown, A. R.; Kuo, W-H.; Jacobsen, E. N. *J. Am. Chem. Soc.* **2010**, *132*, 9286–9288.
19. (a) Xu, H.; Zuend, S. J.; Woll, M. G.; Tao, Y.; Jacobsen, E. N. *Science* **2010**, *327*, 986–990. (b) Uraguchi, D; Ueki, Y; Ooi, T. *Science* **2009**, *326*, 120–123.
20. Bochmann, M. *Acc. Chem. Res.* **2010**, *43*, 1267–1278.
21. (a) Young, W. G.; Winstein, S.; Goering, H. L. *J. Am. Chem. Soc.* **1951**, *73*, 1958–1963. (b) Winstein, S.; Schreiber, K. C. *J. Am. Chem. Soc.* **1952**, *74*, 2165–2170. (c) Winstein, S.; Schreiber, K. C. *J. Am. Chem. Soc.* **1952**, *74*, 2171–2178.

22. Raber, D. J.; Harris, J. M.; Schleyer, P. v. R. In *Ions and Ion Pairs in Organic Reactions* Vol. 2; Szwarc, M., Ed.; Wiley: New York, 1974.
23. (a) De La Mare, P. B. D.; Vernon, C. A. *J. Chem. Soc.* **1954**, 2504–2510 (b) Sreen, R. A. *J. Am. Chem. Soc.* **1960**, 82, 4261–4269. (c) Jia, Z. S.; Ottosson, H.; Zeng, X.; Thibblin, A. *J. Org. Chem.* **2002**, 67, 182–187.
- 24 Smith, M. B.; March, J. *March's Advanced Organic Chemistry*; Wiley, New Jersey, 2007, p 470.
25. Goering, H. L., Blanchard, J. P.; Silversmith, E. F. *J. Am. Chem. Soc.* **1954**, 76, 5409–5418.
26. Goering, H. L.; Silversmith, E. F. *J. Am. Chem. Soc.* **1955**, 77, 1129–1133.
27. (a) Goering, H. L.; Silversmith, E. F. *J. Am. Chem. Soc.* **1955**, 77, 6249–6253. (b) Goering, H. L.; Takahashi Doi, J. *J. Am. Chem. Soc.* **1960**, 82, 5850–5854.
28. Goering, H. L.; Nevitt, T. D.; Silversmith, E. F. *J. Am. Chem. Soc.* **1955**, 77, 5026–5032.
29. (a) Goering, H. L.; Koerner, G. S.; Lindsay, E. C. *J. Am. Chem. Soc.* **1971**, 93, 1230–1234. (b) The importance of conformational factors for 5-methylcyclohex-2-enyl system is demonstrated in: Goering, H. L.; Josephson, R. R. *J. Am. Chem. Soc.* **1962**, 84, 2779–2785.
30. Winstein, S.; Klinedinst Jr., P. E.; Robinson, G. C. *J. Am. Chem. Soc.* **1961**, 83, 885–895.
31. Peters, K. S. *Chem. Rev.* **2007**, 107, 859–873, and references therein.
32. Yabe, T.; Kochi, J. K. *J. Am. Chem. Soc.* **1992**, 114, 4491–4500.
33. (a) Hammett, L. P. *Physical Organic Chemistry*, 2nd ed.; McGraw-Hill: New York, 1970. (b) Bentley, T. W.; Schleyer, P. v. R. *Adv. Phys. Org. Chem.* **1977**, 14, 1–67.
34. Richard, J. P.; Jencks, W. P. *J. Am. Chem. Soc.* **1984**, 106, 1383–1396.
35. Richard, J. P.; Jencks, W. P. *J. Am. Chem. Soc.* **1984**, 106, 1373–1383.

36. (a) Tsuji, Y.; Mori, T.; Richard, J. P.; Amyes, T. L.; Fujio, M.; Tsuno, Y. *Org. Lett.* **2001**, 3, 1237–1240. (b) Teshima, M.; Tsuji, Y.; Richard, J. P. *J. Phys. Org. Chem.* **2010**, 23, 730–734.
37. Schaller, H. F.; Tishkov, A. A.; Feng, X.; Mayr, H. *J. Am. Chem. Soc.* **2008**, 130, 3012–3022.
38. Minegishi, S.; Kobayashi, S.; Mayr, H. *J. Am. Chem. Soc.* **2004**, 126, 5174–5181.
39. For a review on carbocation-nucleophile combination reactions see: Mayr, H.; Ofial, A. R. *J. Phys. Org. Chem.* **2008**, 21, 584–595.
40. For review on solvolysis reactions see: Streidl, N.; Denegri, B.; Kronja, O.; Mayr, H. *Acc. Chem. Res.* **2010**, 43, 1537–1549.
41. (a) Mayr, H.; Ofial, A. R. *Pure Appl. Chem.* **2009**, 81, 667–683. (b) Horn, M.; Mayr, H. *J. Phys. Org. Chem.* **2012**, 25, 979–988.
42. Ammer, J.; Sailer, C. F.; Riedle, E.; Mayr, H. *J. Am. Chem. Soc.* **2012**, 134, 11481–11494.
43. Ammer, J.; Nolte, C.; Mayr, H. *J. Am. Chem. Soc.* **2012**, 134, 13902–13911.
44. Troshin, K.; Schindele, C.; Mayr, H. *J. Org. Chem.* **2011**, 76, 9391–9408.
45. (a) Roos, G. H. P.; Donovan, R. A. *Synlett* **1996**, 1189–1190. (b) Johnson, R.; Sharpless, K. B. In *Catalytic Asymmetric Synthesis*, 2<sup>nd</sup> ed.; Ojima, I, Ed.; Wiley: New York, 2000, pp 231–280.
46. Easton, A. M.; Habib, M. J. A.; Park, J.; Watts, W. E. *J. Chem. Soc., Perkin Trans. 2* **1972**, 2290–2297.
47. (a) Grunwald, E.; Winstein, S. *J. Am. Chem. Soc.* **1948**, 70, 846–854. (b) Bentley, T. W.; Carter, G. E. *J. Am. Chem. Soc.* **1982**, 104, 5741–5747. (c) Kevill, D. N.; D’Souza, M. J. *J. Chem. Res.* **2008**, 61–66.

48. Åkerlöf, G. *J. Am. Chem. Soc.* **1932**, *54*, 4125–4139.

49. The half reaction times were calculated as  $t_{1/2} = (\ln 2)/k$  where  $k$  is the pseudo-first-order rate constant obtained by fitting  $[(R)\text{-}\mathbf{1}]_t$  to the monoexponential function  $\ln [(R)\text{-}\mathbf{2}]_t = -kt + \text{const.}$  In the case of 90% aq acetone, only first 40 h of the reaction were evaluated because re-isomerization of **2** which is formed during the reaction causes upward drifts in the  $\ln[(R)\text{-}\mathbf{1}]_t$  vs.  $t$  plot (see Supporting Information for details).

50. As discussed in detail below, equation 11 predicts a second-order rate constant of  $1.5 \times 10^9 \text{ M}^{-1} \text{ s}^{-1}$  for the reaction of cation **6** with piperidine ( $N = 18.44$ ,  $s_N = 0.44$  for piperidine in water and  $E = 2.70$  for **6**). An up-to-date database of reactivity parameters  $E$ ,  $N$ , and  $s_N$  can be found at [www.cup.lmu.de/oc/mayr/DBintro.html](http://www.cup.lmu.de/oc/mayr/DBintro.html).

51. Whereas 1,6-dibenzyl-1,2,3,4,5,6-hexahydro-1,3a,6,8-tetraazaphenalene was found to be the most universal photoleaving group among a series of variously substituted aminopyridines (Nigst, T. A; Ammer, J.; Mayr, H. *J. Phys. Chem. A* **2012**, *116*, 8494–8499), its non-benzylated analogon can also be used as well in the present case, as the Lewis acidity of cation **6** is high enough to form stable pyridinium salts with both pyridines.

52. Goering and Winstein differentiate between *external return*, i.e., the reaction between an added common anion and the free or paired carbocation, which results in the isotope exchange between the substrate and  $^{14}\text{C}$  labeled 4-nitrobenzoic acid, and *external ion pair return*, i.e., recombination of the solvent-separated ion pair, which can be suppressed by the addition of strong nucleophiles but does not result in the exchange with isotope-labeled 4-nitrobenzoic acid. As the participation of the SSIPs does not play a significant role in the present case, effects related to *external ion pair return* will be neglected.

53. Dvorko, G. F.; Ponomareva, E. A. *Russ. J. Gen. Chem.* **2010**, *80*, 1615–1625, and references therein.

54. Kantner, S. S.; Humski, K.; Goering, H. L. *J. Am. Chem. Soc.* **1982**, *104*, 1693–1697.
55. Thibblin, A. *J. Chem. Soc., Perkin. Trans. 2* **1987**, 1629–1632.
56. Tsuji, Y.; Richard, J. P. *Chem. Rec.* **2005**, *5*, 94–106.
57. The detailed description of the evaluation procedure can be found on pages S72–S109 of the Supporting Information.
58. McClelland, R. A.; Kanagasabapathy, V. M.; Banait, N. S.; Steenken, S. *J. Am. Chem. Soc.* **1989**, *111*, 3966–3972.
59. Denegri, B.; Minegishi, S.; Kronja, O.; Mayr, H. *Angew. Chem., Int. Ed.* **2004**, *43*, 2302–2305.
60. Mayr, H.; Bug, T.; Gotta, M. F.; Hering, N.; Irrgang, B.; Janker, B.; Kempf, B.; Loos, R.; Ofial, A. R.; Remennikov, G.; Schimmel, H. *J. Am. Chem. Soc.* **2001**, *123*, 9500–9512.
61. Atkins, P.; de Paula, J. *Atkins' Physical Chemistry*, 9<sup>th</sup> ed.; Oxford University Press: Oxford, 2010, p 840.
62. More decimals of  $k_{-1}/k_2$  and  $k'_{-1}/k_2$  than given in Scheme 5 were used.
63. While we do not have quantitative evidence for this assumption, picosecond dynamics of laser flash photolytically generated carbenium ions provide qualitative confirmation of it, as the ratio of rates of geminate recombination (corresponding to  $k_{-1}$ ) and diffusional separation (corresponding to  $k_2$ ) of photolytically generated ion pairs was reported to increase with increasing reactivity of the carbocation in the ion pair (see refs 32 and 42).
64. Sailer, C.; Ammer, J.; Riedle, E.; Mayr, H.; unpublished results.
65. It should be noted that  $p_{\text{ER}}$  reflects the probability that a free carbenium ion **10** is captured by <sup>−</sup>OPNB and not by the solvent. The probability that CIP generated by ionization of **10**-OPNB gives rise to a rearranged product via external return (e.g., (*S*)-**10**-OPNB from (*R*)-**10**-OPNB) is given by  $0.5(1 - p_{\text{IR}}/100\%)p_{\text{ER}}$ . This expression subtracts the fraction of CIPs

consumed by internal return and multiplies with 0.5 to account for the fact that in the case of symmetrical allyl cations 50% of external return regenerates the starting material. As  $p_{\text{IR}}$  and  $p_{\text{ER}}$  do not correspond to competing processes, the sum of these terms can also be greater than 100%.

66. Minegishi, S.; Loos, R.; Kobayashi, S.; Mayr, H. *J. Am. Chem. Soc.* **2005**, *127*, 2641–2649.

67. Goering, H. L.; Pombo, M. M.; McMichael, K. D. *J. Am. Chem. Soc.* **1963**, *85*, 965–970.

68. Troshin, K.; Mayr, H.; Mayer, P. *Acta Crystallogr., Sect. E: Struct. Rep. Online* **2012**, *68*, o2549.

69. Hayashi, T.; Yamamoto, A.; Yoshihiko, I.; Nishioka, E.; Miura, H.; Yanagi, K. *J. Am. Chem. Soc.* **1989**, *111*, 6301–6311.

70. De Rycke, N.; Berionni, G.; Couty, F.; Mayr, H.; Goumont, R.; David, O. R. P. *Org. Lett.* **2011**, *13*, 530–533.

## TOC Graphic

